Ground Motion and Seismicity Aspects of the 4 September 2010 Darfield and 22 February 2011 Christchurch Earthquakes

Technical Report Prepared for the Canterbury Earthquakes Royal Commission

Brendon A. Bradley[1,2]

[1]Director, Bradley Seismic Limited

[2]Lecturer, Department of Civil and Natural Resources Engineering, University of Canterbury

13 January 2012

Christchurch, New Zealand

Disclaimer:

This report has been commissioned by the Canterbury Earthquakes Royal Commission to provide information on ground motions and seismicity related to the Canterbury earthquakes. The authors accept no liability for the use of the material contained in this document by third parties.

Table of Contents

Executive Summary

The 22 February 2011 and 4 September 2010 earthquakes caused strong ground motions in the densely populated Christchurch and surrounding Canterbury region, and consequently resulted in the largest earthquake damage in New Zealand's history since European settlement. The ground motions caused complete and partial collapse of many commercial, residential and industrial structures, and severe liquefaction of surficial soils over large regions caused extensive damage to infrastructure, and lifelines.

The process of earthquake occurrence and the consequent ground motions that they produce are extremely complex. While earthquake-induced ground motion can be violent and result in substantial damage in seconds, the underlying physical processes which cause earthquakes evolve over geologic time scales, and therefore the present knowledge of the earthquake process (and therefore earthquake-induced ground motions) is limited. As a result, seismicity and ground motion modelling requires dealing with a paucity of data, and high uncertainties, in order to forecast the likelihood of earthquakes and strong ground motions in a specific region over a specific period of time.

Earthquakes in the Canterbury sequence occurred on unmapped faults, which were not specifically recognised prior to the events. However, such 'off-fault' earthquakes are accounted for in 'background seismicity' within seismicity models. The maximum magnitude of background earthquakes which can occur off known faults was $M_w 7.0$ in the seismicity model underlying NZS1170.5:2004, but in the current model is $M_w 7.2$. That is, all earthquakes in the Canterbury sequence are of a size that is within that provided by the current New Zealand seismicity model. However, the Canterbury earthquakes have often occurred at shallow depths, lower than the minimum depth of 10km in the current New Zealand seismicity model. The current seismicity model also treats background earthquake sources as 'point-sources', which is inconsistent with ground motion models which represent the finite nature of the earthquake fault. Both the 'point-source' assumption and minimum depth of 10km result in the current New Zealand seismicity model providing un-conservative estimates of ground motion intensities in the near-source region of shallow 'background' earthquakes, such as those in the Canterbury earthquake sequence.

As a result of a dense instrumentation network, a vast array of strong ground motions has been recorded in the Canterbury earthquake sequence. Comparison of the observed ground motions with the ground motion model conventionally used in New Zealand seismic hazard analysis, in particular that underpinning NZS1170.5:2004, illustrates that the model contains several notable deficiencies. In particular, this model provides a significant over-estimation of response spectral amplitudes at short vibration periods ($T \approx 0.2s$) and also a significant under-estimation at moderate-to-long vibration periods for ground motions in the near-source region of the causal earthquake. A recently developed New Zealand-specific model, based on a significantly larger set of empirical ground motions, provides a significantly more consistent prediction when compared with the observed ground motions (particularly at short and moderate periods). Nonetheless, at long periods, forward directivity, basin-induced surface waves, and nonlinear response of surficial soils are prevalent in some of the strong ground motion, which are either not explicitly modelled, or poorly constrained by empirical models. Observations illustrate that that the NZS1170.5:2004 factor for forward-directivity effects is largely un-conservative and requires revision, as does the currently oversimplified relationship for determination of vertical ground motion spectra. The broad site classification scheme, as currently prescribed in

NZS1170.5:2004, is too simplistic to be able to ascertain the significance of nonlinear site effects with accuracy or precision.

1. Introduction

The Canterbury earthquake sequence, which began in September 2010 and continues today, has included numerous signficant earthquakes which have adversely affected the region. These earthquakes produced ground motion intensities equal to, and exceeding, those for which modern structures are designed for in Christchurch and its central business district (CBD). Consequently, such events resulted in substantial damage to buildings, infrastructure, and lifelines. The 22 February 2011 earthquake was particularly damaging, and resulted in 182 fatalities principally from the complete or partial collapse of several commercial structures. As a result of the strong ground motions, nonlinear response of surficial soils and, in particular, severe liquefaction occurred over large regions of Christchurch, particularly to the east of the CBD.

This report provides an examination of seismicity and ground motion aspects on arguably two of the most signficant earthquakes, those on the 4 September 2010 and the 22 February 2011. The concepts of seismic hazard analysis and design ground motions are presented to provide the necessary context for an essential understanding of seismicity and ground motion models, which underpin design ground motion provisions in the New Zealand Seismic loadings standard, NZS1170.5:2004. The consistency of relevant New Zealand seismicity models are then examined with respect to the Canterbury earthquakes which have occurred. Finally, the observed strong ground motions are compared with empirical New Zealand-specific ground motion models. Recommendations for modifications to seismicity and ground motion models are provided based on the observations. This report contains technical information, but an attempt has been made provide a physically oriented focus, and to structure the presentation of material such that it is digestible for a general audience.

2. Seismic Hazard Analysis and Design Ground Motions

The predominant cause of earthquake-induced damage is that resulting from earthquake-induced strong ground motion (or simply 'ground motion' for brevity). Assessment of the ground motion hazard posed to structures, whether it be cast within a probabilistic of deterministic framework comprises the two key tasks of: (i) seismicity modelling; and (ii) ground motion modelling. These two tasks are outlined below followed by an explanation of seismic hazard analysis and how design ground motions are subsequently obtained.

2.1. Seismicity Modelling

Seismicity modelling involves assessment of the location, size, and frequency/likelihood of earthquakes. Because earthquakes cannot be predicted, then seismicity models are typically probabilistic (giving probabilities of earthquake occurrence within a given time interval), and therefore commonly referred to as 'earthquake forecasts'.

Because instrumental records of earthquake occurrence are short, relative to the recurrence intervals of earthquakes on specific faults, it is not possible to develop a useful seismicity model on the basis of observational data alone (in the manner in which flood hazard is often assessed, for example). As a result, in order to maximise available data and theories, seismicity modelling conventionally incorporates geologic, geodetic, and instrumental seismology data.

Geologic information is typically utilized to ascertain specific locations of major active faulting and their fault geometry (i.e. fault length). Paleo-seismologic information from geologic sediments and rocks at the locations of inferred faults are also often utilized to estimate other characteristics of the faults, such as fault deformation (e.g. slip rate). Empirical methods, termed magnitude-scaling relations, are conventionally used with the inferred fault geometry to compute the likely magnitudes which such faults could produce if a 'characteristic' earthquake [1] was to occur on the fault, in which the full fault plane ruptures. If it is assumed that faults are characteristic in nature then based on the characteristic earthquake magnitude, fault geometry and deformation characteristics, an average recurrence interval (defining the average time between characteristic ruptures of the fault) can be computed. If it is assumed that an earthquake fault is fractal (i.e. produces earthquakes of all magnitudes) and obeys the Gutenberg Richter relationship [2], then the recurrence intervals of the various magnitude of concern can also be computed. Within the scientific community there remain arguments for and against both the Characteristic and Gutenberg-Richter magnitude–frequency distributions at present [3, 4]. The New Zealand seismic hazard model [5, 6] assumes all faults are characteristic in nature, so that large earthquakes occur periodically. However, smaller 'background' earthquakes, discussed in the following paragraph, are considered to follow a Gutenberg-Richter magnitude-frequency distribution.

Geological evidence at the earth's surface is often not discernable for active faulting which produces small-to-moderate magnitude earthquakes, and/or faulting with a relatively long recurrence interval between signficant earthquake events. Therefore, in addition to seismic hazard resulting from geologically defined active faulting, spatially varying 'background' seismicity is also often included in a seismicity model. For example, the New Zealand Seismic Hazard Model [5, 6] utilizes background seismicity to account for earthquakes of magnitudes less than $M_w 6.0$, which are considered to not be adequately represented within the geologically determined fault-based component of the seismicity model. Background seismicity is conventionally obtained based on the Gutenberg Richter distribution of historically recorded instrumental seismicity. Based on the statistics of the observed historical seismicity the spatial distribution of frequencies of 'background seismicity' can be determined.

Geodetic information such as global plate boundary slip rates can be used to provide additional constraint to a seismicity model comprising fault-based and background seismicity. The use of real-time geodetic information in seismicity modelling is not well established, and is a topic of current research.

2.2. Ground Motion Modelling

As previously mentioned, structures are designed to resist earthquake-induced ground motions, not to resist earthquakes themselves. The aim of ground motion modelling is to determine the ground motion, at a specific location as a result of a future earthquake which is forecast as part of the seismicity modelling discussed previously.

Ground motion modelling can be conducted in various manners, and primarily depends on whether one desires an estimate of the full acceleration-history of ground motion, or whether simple ground motion intensity measures (e.g. scalar quantities such as peak ground acceleration, PGA, or pseudo-spectral acceleration, SA) are desired. Conventional seismic design is based on the response spectral amplitudes of a ground motion (e.g. SA). Advanced methods of structural and geotechnical analysis require the full ground motion acceleration-history, but methods for obtaining such acceleration histories are not discussed herein.

For the purpose of determining ground motion intensity measures, (e.g. SA), for seismic design, empirical ground motion prediction equations (GMPEs) are conventionally employed. Such GMPEs are mathematical functions derived based on historically recorded ground motions. Such functions are empirical in nature, and therefore should be considered as only representative for use in modelling ground motion for scenarios which are well represented by the database of historically recorded ground motions. Unfortunately, as a simple result of the fact that moderate-to-large earthquakes occur infrequently, and that strong motion instrumentation must be in-place to record the ground motions from such events, there is a paucity of recorded strong motions from such events, particularly at close source-to-site distances (which are the situations which are most relevant for seismic design of structures).

Because of the complexity of the process of earthquake rupture, wave propagation, and local effects of the surficial soils directly beneath the site, the characteristics of ground motions as predicted by empirical GMPEs are highly uncertain. As a result it is conventional that a GMPE is a probabilistic function of the predictor variables (e.g. earthquake magnitude, source-to-site distance, local soil conditions etc). An example of such a GMPE, and its uncertainty, is given in Figure 1, which compares the prediction and observation at Christchurch Hospital (CHHC) during the 22 February 2011 Christchurch earthquake. It can be seen that the uncertainty in the prediction is significant. For example, at a vibration period of 1.0s, the median prediction is SA(1s)=0.8g, while the 16^{th} and 84^{th} percentiles are 0.45g and 1.4g, respectively.

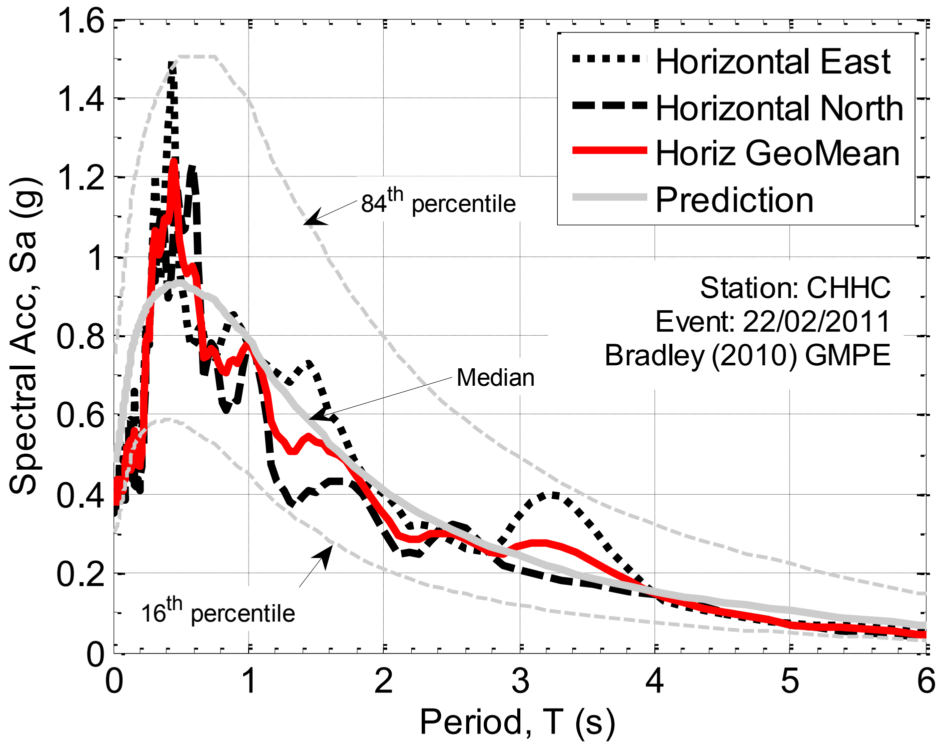

Figure 1: Comparison of the pseudo-acceleration response spectra (SA) observed at Christchurch Hospital (CHHC) during the 22 February 2011 Christchurch earthquake (both North and East components, and the geometric mean) with the empirical (geometric mean) prediction based on the NZ-specific Bradley [7] model. Note in particular the large uncertainty in the prediction as indicated by the differences between the median, 16th, and 84th percentiles of the prediction.

2.3. Deterministic Seismic Hazard Analysis (DSHA)

A deterministic seismic hazard analysis (DSHA), or scenario-based seismic hazard analysis, is predicated on the determination of earthquake-induced ground motion at a site given that the considered seismic sources will cause earthquakes in the service life of the structure [8]. Thus, the result of a DHSA is the ground motion (or ground motion intensity measure(s)) which is expected to occur given that the scenario earthquake occurs. In order to account for the multiple earthquake sources which pose a seismic hazard at the site of interest, the ground motion expected as a result of earthquakes on each potential earthquake source is computed, and the maximum ground motion is taken as the final result.

The benefits of DSHA is that it is conceptually simple, something which cannot not be under-emphasised. The main drawback of DSHA is that the likelihood of earthquake sources rupturing in the service life of the structure, and also the uncertainty in the ground motion prediction are not explicitly considered. That is, a DSHA might state that: “At site X the controlling seismic source will produce a ground motion with a median of 0.5g PGA and lognormal standard deviation of 0.6, and this seismic source is inferred to rupture on average every 1000 years”. Thus the analyst can ascertain that for a structure with a typical service life of 50-100 years, the likelihood of the earthquake occurring is relatively low (approx 5-10%), and if this earthquake does occur the ground motion will likely have a PGA of approximately 0.5g PGA, and 16th and 84th percentiles are 0.30 and 0.82g, respectively. However, the likelihood of the earthquake occurring, and the consequent ground motion expected are not explicitly combined. Therefore, determining a single design value requires the discretion of the analyst that the likelihood of the governing scenario earthquake is reasonable (i.e. not too conservative), and that the percentile of the ground motion amplitude selected for design, given the event occurs, is compatible with the level of risk tolerated.

In order to subsequently compare with probabilistic seismic hazard analysis (PSHA) discussed in the next section, it is useful to write a DSHA in the following steps:

- For each earthquake rupture scenario, Rup_i, considered, compute the distribution of the ground motion intensity measure (IM) of interest, $f(IM|Rup_i)$.
- Specify the percentile of the ground motion uncertainty to consider so that a deterministic ground motion intensity value for the given rupture scenario can be obtained. This value may be denoted as $IM^*|Rup_i$. For example, it is common to choose the 84th percentile [8, 9], so there is only a 16% chance that if the earthquake occurs, the ground motion will exceed the design value.
- Determine the controlling scenario as the maximum of all considered scenarios, that is: $IM^*_{design} = \max_i(IM^*|Rup_i)$. This is then used as the design ground motion intensity.
- Repeat the above three steps for different ground motion intensity measures of interest (e.g. SA values for different vibration periods).

2.4. Probabilistic Seismic Hazard Analysis (PSHA)

Probabilistic seismic hazard analysis (PSHA) has several major differences from DSHA: (i) the likelihood of the earthquake source rupturing during the considered time period is explicitly considered; (ii) the uncertainty in the ground motion prediction is explicitly considered; and (iii) the hazard from different seismic sources are additively combined to obtain a 'total' site hazard.

Unlike DSHA, PSHA is performed in a probabilistic framework with the result being a probability distribution describing the likelihood that a given value of ground motion intensity will be exceeded in a given time period. Therefore, for each value of ground motion intensity considered, ($IM=im$), the following steps are required:

- For each earthquake rupture scenario considered, compute the distribution of the ground motion intensity measure of interest, $f(IM|Rup_i)$. Determine the probability that $IM>im$, $P(IM > im|Rup_i)$, and multiply by the mean annual rate of occurrence of the earthquake rupture scenario, $\lambda(Rup_i)$ to obtain the mean annual rate at which Rup_i occurs and produces a ground motion with $IM>im$.
- By assuming each earthquake rupture is independent compute the mean annual rate of $IM>im$ from all potential earthquake ruptures ($N_{ruptures}$) by summing the contribution from individual ruptures.

The formal equation for PSHA can thus be written as:

$$\lambda(IM > im) = \sum_{i=1}^{N_{ruptures}} P(IM > im|Rup_i)\lambda(Rup_i) \tag{1}$$

As previously noted, since Equation (1) is a function of the value of IM selected, then different values are obtained for different ground motion intensities. A plot of $\lambda(IM > im)$ for a range of IM values is referred to as a ground motion hazard curve. Figure 2 provides an example of a hazard curve of SA(1.5s). Because the hazard curve is highly skewed, it is conventional to plot it on a log-log plot.

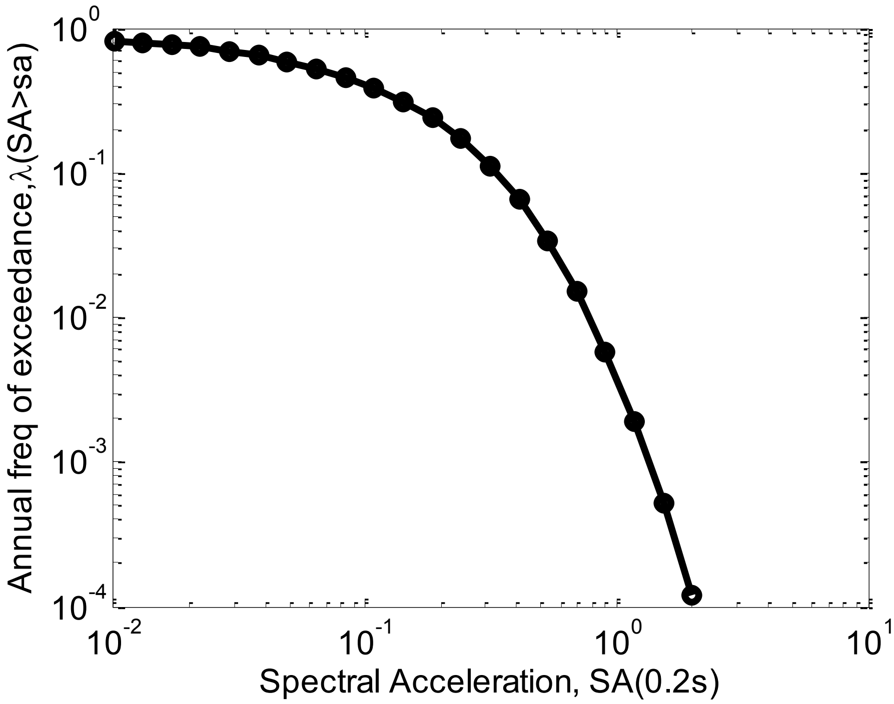

Figure 2: Ground motion hazard curve for pseudo-spectral acceleration at a period of 0.2s, SA(0.2s).

Based on the assumption that earthquake occurrence is a random Poisson process [10], the probability of exceedance of a particular ground motion intensity level, $P(IM > im)$, in a given time period, T, can be computed from the annual frequency of exceedance, $\lambda(IM > im)$. Specifically:

$$P(IM > im) = 1 - \exp(-\lambda T) \tag{2}$$

where exp () is the exponential function. Thus for a service life of 50 years, a 10% probability of exceedance is equivalent to an annual exceedance frequency of $\lambda = 2.1 * 10^{-3}$. Another metric to quantify likelihood of occurrence is the return period, R, defined as the inverse of the annual frequency, e.g. $R(IM > im) = 1/\lambda(IM > im)$. Thus a return period of 500 years corresponds to an annual frequency of exceedance of $\lambda(IM > im) = \frac{1}{500} = 0.002$. From Figure 2, the ground motion intensity for this return period is approximately SA(0.2s)=1.2g.

With respect to the previously identified deficiencies of DSHA we can see that for PSHA:

- The likelihood that a potential earthquake source ruptures, $\lambda(Rup_i)$, is explicitly considered in Equation (1), in contrast to DSHA, where it must be implicitly considered.
- The uncertainty in the estimation of ground motion intensity given the occurrence of an earthquake is explicitly considered in Equation (1) via the term $P(IM > im|Rup_i)$.

- The effects of multiple earthquake sources are combined using the total probability theorem (i.e. the summation in Equation (1)).

Hence, based on the above points one may consider that PSHA is superior to DSHA. However, the rigorous treatment of uncertainty in PSHA also provides several additional problems which require careful consideration:

- **Controlling Earthquake Scenario:** The seismic hazard curve resulting from PSHA alone has no concept of a controlling earthquake scenario. For example, if the design ground motion is selected as the value corresponding to a 500 year return period, then a hazard curve provides only a corresponding value of the design ground motion (e.g. SA(0.2s)=1.2g in the case of Figure 2), but no information on which earthquake sources produce this hazard level. While this problem can be remedied by seismic hazard deaggregation, which provides the contribution of a given hazard curve value from various potential earthquake sources, such deaggregations are not available in seismic design guidelines, such as NZS1170.5:2004, and are therefore no available for conventional design. Such information is only available if a site-specific seismic hazard analysis is performed, and this is typically beyond the scope of conventional structural design at present due to the costs to perform or subcontract such analyses.

- **Frequency of exceedance for design:** In order to use the seismic hazard curve to obtain a single design ground motion intensity, the analyst must specify a probability of exceedance, return period, or frequency of exceedance. This is akin to having to specify a percentile of the scenario ground motion intensity distribution in DSHA.

As a result of these additional complexities entailed with PSHA, it is the author's opinion that DSHA and PSHA provide different information, both of which are insightful, and should therefore be considered as two methodologies which provide complementary information for the design of structures [11].

2.5. Design Ground Motions

In New Zealand, as per NZS1170.5:2004, and generally internationally, it is common to determine design ground motion intensities predominantly via the results of PSHA, with supplementary results from DSHA used to provide upper and lower bounds.

2.5.1. Elastic Response Spectra

One way in which the results of PSHA for spectral accelerations, SA, can be expressed in a compact manner is to create a uniform hazard spectrum (UHS). A UHS represents a locus of spectral accelerations at various vibration periods which have the same annual frequency of exceedance. A schematic illustration of the calculation prodecure for a UHS is shown in Figure 3. It is important to note that since the SA values on a UHS are obtained from separate PSHA's (for different vibration periods), then the contribution of different earthquake scenarios is different at these different vibration periods. Because of the manner in which strong ground motion varies with earthquake magnitude and source-to-site distance, it is common that short-period SA values of a UHS are dominanted by relatively moderate earthquake magnitudes at relatively short source-to-site distances, while long-period SA values of a UHS are dominated by relatively large earthquake magnitudes at relatively large source-to-site distances. This variation in dominant scenario with vibration period is often not well understood.

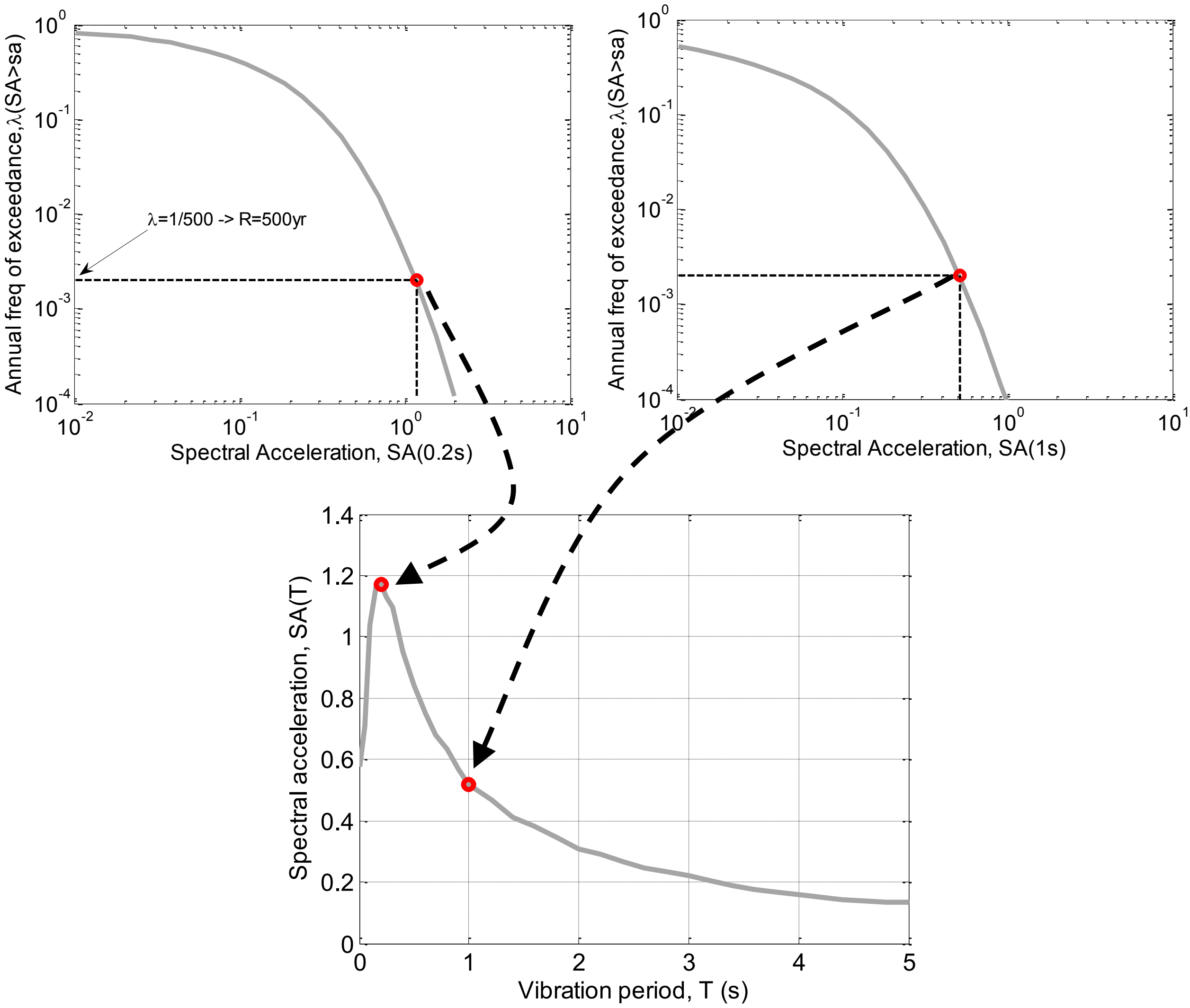

Figure 3: Illustration of the process of creating a uniform hazard spectrum from the results of probabilistic seismic hazard analysis (PSHA), for a return period of $R = 500$ *years.*

In NZS1170.5:2004, a 'codified' version of a normalized uniform hazard spectrum is provided (the 'C_h' factor), which is obtained based on examination and interpretation of UHS computed at multiple locations in New Zealand. The normalized UHS in NZS1170.5:2004 is a function of the local soil conditions, as soft soils have the potential to cause signficantly larger long period ground motion than rock and stiff soil sites (e.g. see section 4.3.3). By multiplying the normalized uniform hazard spectrum by a scale factor, Z, to represent the seismic activity of the region, NZS1170.5:2004 provides an approximation of the 500-year return period UHS for the region of interest.

Since the hazard curve covers a continuum of IM values then ideally the design of the structure should make use of multiple IM values. As these different IM values have different likelihoods of occurrence then different performance expectations could be prescribed for each as a function of the societal importance of the structure. In NZS1170.5:2004, the return period factor, R, is used to multiply the 500-year return period UHS to obtain an approximate UHS for different return periods. Hence by definition, $R = 1$, for a return period of 500 years.

In addition to the increase in ground motion intensity at long vibration periods which can occur at soft soil sites, strong long period ground motion can also occur as a result of forward-directivity effects which result from the superposition of seismic waves in the near-source region. In NZS1170.5:2004, near-fault forward directivity effects are partially accounted for using a near-fault factor, *N*, which varies as a function of distance from the site of interest to a major fault, and vibration period of interest.

By combining all of the aforementioned features, the elastic design response spectral acceleration (SA) from NZS1170.5:2004 can be computed as:

$$C(T_1) = C_h(T_1) * Z * R * N \tag{3}$$

where T_1 is the first-mode period of the structure considered.

2.5.2. Inelastic Response Spectra

The elastic design response spectra examined in the previous section represents the design spectral acceleration that is required for a structure which is intended to remain linear elastic under the design ground motion intensity. It is conventional to accept controlled nonlinearity to occur in structures during strong ground motion because: (i) it can sometimes be economically prohibitive to design a structure to remain elastic under strong ground motion; and (ii) the consequences, in terms of structural damage and disruption, of limited nonlinear response can sometimes be acceptable, given the likelihood of the design ground motion occuring in the life of the structure.

In NZS1170.5:2004, inelastic response spectra can be obtained from the elastic response spectra from the following equation:

$$C_d(T_1) = \frac{C(T_1)S_p}{k_\mu} \tag{4}$$

where C_d is the inelastic response spectral ordinate; S_p the structural performace factor [12]; and k_μ is a ductility reduction factor. The ductility reduction factor, k_μ, in particular, is a simple function of the design displacement ductility, μ (representing the amount of nonlinearity occuring), and the vibration period, T_1, based largely on the work of Velestos and Newmark [13] and Newmark and Hall [14].

Carr [15] provided a comparison of constant ductility inelastic and elastic (i.e. $\mu = 1$) response spectra of ground motions from the 22 February 2011 Christchurch earthquake. The results demonstrated that the 'equal displacement approximation' which undelies the ductility reduction factor for moderate-to-long vibration periods (i.e. $T_1 > 0.7s$ for soil classes A-D) is an imprecise approximation. It should be noted that the equal displacement approximation as proposed by Velestos and Newmark [13] has always been known to be a coarse approximation (the scatter in the approximation varies between a factor of 0.4 and 1.6 in Figure 6 of Velestos and Newmark [13]). As a result, other seismic design guidelines such as the Architectural Institute of Japan employ the more conservative 'equal-energy approximation'. Clearly, as demonstrated from the results of Carr [15], the use of the equal displacement approximation in seismic design guidelines requires revision.

In light of the comments above, inelastic spectra of observed ground motions should be compared with the inelastic design spectra when attempting to assess the performance of a specific structure as compared with the designed performance expectations (since the error in the displacement reduction factor may result in errorenous performance comparisons when using the observed and design elastic response spectra). However, as the emphasis of this report is on seismicity and ground motions, rather than the response of specific inelastic structures, further details on inelastic response spectra are not given here and attention is restricted to elastic response spectra.

2.6. Scrutinizing Seismic Hazard Analyses with Earthquake and Ground Motion Observations

Following an earthquake event it is natural that assessments are made to examine the adequacy of current seismic design provisions and their underpinning methodologies. For structural and geotechnical engineers, assessments may involve the intensity of the observed ground motion with the design ground motion intensity and subsequently comparison of the observed and expected performance of structures. From an engineering seismology perspective, it is also desired to assess the earthquake and ground motion characteristics and compare them with predictive models, seismic hazard analyses, and design seismic intensities.

Comments are often made that observed ground motions that exceed the design seismic intensities provide evidence that the design seismic intensities are flawed, as a result of flawed inputs, or a flawed methodology. However, when attempting to reconcile observations with design values it is necessary to understand how the design values are obtained. For example, previous sections have demonstrated that a PSHA is obtained by summing over all of the potential earthquake sources which contribute a ground motion hazard for the site considered, including the likelihood of the earthquake source rupturing and uncertainty in the ground motion prediction. Hence comparison of the results of a PSHA with an observed ground motion, which is produced from a single earthquake source, that has occurred, is strictly incorrect. As previously noted, a direct comparison of observed ground motion and design ground motion intensities should be performed only for the purpose of assessing the observed and expected seismic performance of structures.

In order to scrutinize seismic hazard analyses (either probabilistic or deterministic) based on a single earthquake and its observed ground motions it is necessary to compare the observations with the predictive models which are inputs to a DSHA and PSHA, namely: (i) the seismicity model; and (ii) the ground motion prediction equation (GMPE). It must also be borne in mind that the causal earthquake(s) and its/their recorded ground motion(s) represent merely a sample (often small) from the seismicity and ground motion models, and therefore caution must be exercised to ensure that over-interpretation of the results is avoided. In the following sections, the characteristics of the seismicity model and GMPE's are scrutinized relative to observations from the Canterbury earthquakes.

3. The New Zealand Seismicity Model and the Canterbury Earthquakes

3.1. Consistency of the New Zealand Seismicity Model

A seismicity model, in a general sense, provides the location, size, and frequency of earthquakes in a particular region. Therefore scrutinizing a seismicity model based on an observed earthquake should consider the following fundamental question:

- Does the seismicity model allow for the possibility of an earthquake to occur at the observed location and of the observed magnitude?

It should be noted, in particular, that the 'frequency' aspect of a seismicity model represents a probabilistic quantity, and hence this cannot be explicitly scrutinized based on the deterministic occurrence of an earthquake. Following the above fundamental question, there are various additional secondary questions which can be posed, for example:

- Does the fault along which the earthquake occurred have the same fault geometry (e.g. strike, depth, length, width, dip) as that in the seismicity model?
- Is the fault deformation (e.g. slip rake angle, slip magnitude along the fault, surface rupture length, surface rupture displacement etc). consistent with that in the seismicity model? (not all of these quantities may be part of a conventional seismicity models, but part of fault rupture hazard models).

None of the fault structures which have ruptured in the Canterbury earthquake sequence have occurred on known active faults which form the fault-based component of seismicity in the New Zealand seismicity models. However, this does not imply that the model is deficient, as it should be recalled that 'off-fault' seismicity is also accounted for via background seismicity sources. The following paragraphs therefore compare the characteristics of the earthquake ruptures in the Cantebrury earthquake sequence with those of the background seismicity component of New Zealand seismicity models.

Design ground motion intensities in NZS1170.5:2004 are based on seismic hazard analyses using the seismicity model of Stirling et al. [6]. For the Canterbury region in which the Canterbury earthquake sequence has occurred, the background seismicity model of Stirling et al. [6] allows for the possibility of background earthquakes of reverse-faulting mechanism to occur with magnitudes up to $M_w7.0$. These same background details were also used in a Canterbury-specific seismic hazard update in 2007 [16]. Hence, it may be argued that the 4 September 2010 Darfield earthquake ($M_w7.1$, predominantly strike-slip deformation) is not strictly accounted for in the seismic hazard analyses that underpin NZS1170.5:2004, and the most up-to-date hazard analysis at the time of the event. It is worthy of note however that the 2010 update of the Stirling et al. [6] model allowed for background earthquakes in the Canterbury region of up to $M_w7.2$ [5]. While this updated model [5], assigns that background earthquakes are reverse-mechanism (compared with the Darfield earthquake being a strike-slip mechanism), this should be considered as conscious conservatism since reverse-faulting earthquakes tend to produce systematically larger ground motions than strike-slip and other faulting styles. With the exception of the 4 September 2010 earthquake, events in the Canterbury earthquake sequence have been at, or below, $M_w6.3$, and therefore the size of these events is adequately captured by seismicity models, both up-to-date and those which underpin NZS1170.5:2004.

The background seismicity models of Stirling et al. [5, 6, 16] consider background earthquakes as point sources located at depths of 10, 30, 50, 70, and 90 km. Events in the Canterbury earthquake sequence have had centroid depths (the 'centre of radiated energy') which are notably shallower than that minimum background depth of 10km. All other things equal, shallow earthquakes result in stronger ground motions at the earth's surface as a result of smaller geometric spreading attenuation, which is principally a function of the distance from the earthquake source to the site of interest. Therefore, the depths of background seismicity are unconservative in the current seismicity models, and should be revised to account earthquakes with shallower centroid depths. This could be achieved in a deterministic manner (i.e. calculating rates for background earthquakes at fixed, but shallower, depths), or probabilistically (i.e. setting the centroid depth of shallow earthquakes as a random variable, with a distribution based on observational data).

Even for small-to-moderate earthquake events, the finite size of the fault plane is important in ground motion prediction at locations in the near-source region. It was noted in the previous paragraph that background earthquakes are treated as point sources in New Zealand seismicity models. However, ground motion prediction equations (GMPEs) use finite-fault source-to-site distance metrics to quantify geometric spreading effects. For example, while the centroid depth of the 22 February 2011 Christchurch earthquake had a centroid depth of 4km, it is inferred to have a fault plane with significant slip at depths as low as 1km [17]. Similarly, while the 4 September 2010 Darfield earthquake had a centroid depth of 8km, it resulted in surface rupture and therefore has a finite fault depth of 0km. The same ideas also apply for consideration of the fault plane in the horizontal direction, for example, the centroid of the 4 September 2010 Darfield earthquake is approximately 35km from central Christchurch, as compared to the nearest distance on the fault plane being only 14km. As finite-fault source-to-site distances are always less than their respectively point-source-to-site distances then the point source representation of background seismicity in the current New Zealand seismicity models provides un-conservative seismic hazard estimates. Noting that finite-fault details for background seismicity sources are not known in the manner that they are for fault-based seismicity, then finite fault details of background seismicity sources should be considered with geometrical parameters (dip, strike etc.) either deterministically estimated, or probabilistic distributions provided.

In order to illustrate the significance of the un-conservatism resulting from a minimum depth of 10km, and the assumption of point sources for background seismicity, it is insightful to consider how these affect the predicted ground motions in the earthquake events that have occurred. Figure 4 illustrates the predicted median response spectrum amplitudes at Christchurch Hospital (CHHC) from the 22 February 2011 and 4 September 2010 earthquakes. The predictions are based on the New Zealand-specific Bradley [7] GMPE, whose performance is examined subsequently in section 4.2. Figure 4 illustrates the predicted response spectra assuming: (i) that the earthquake depth is 10km and that the earthquake is a point source (what current New Zealand seismicity models [5, 6, 16] consider); (ii) that the earthquake depth is equal to the calculated event-specific centroid depth, but still a point source; and (iii) the correct consideration of the earthquake geometry by using its finite fault. It can be seen that, as previously noted, approaches (i) and (ii) provide an un-conservative estimate of the ground motion as compared to the consistent approach of representing earthquakes as finite faults in seismicity modelling. The reason for the difference in the response spectra is a result of the different source-to-site distance, R_{rup}, which is input into the ground motion model as annotated.

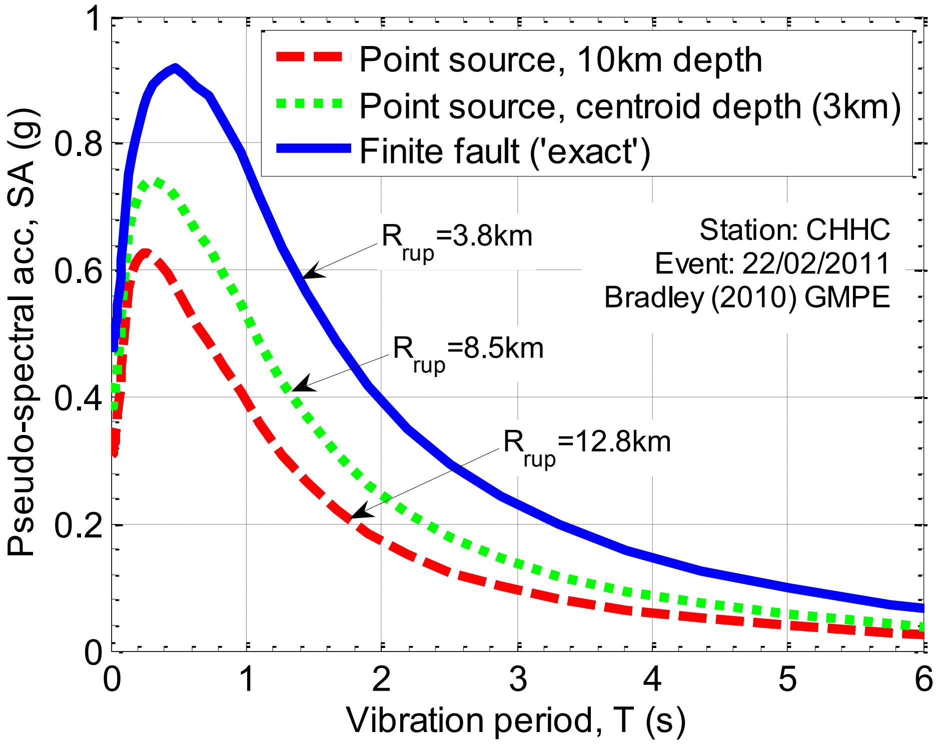

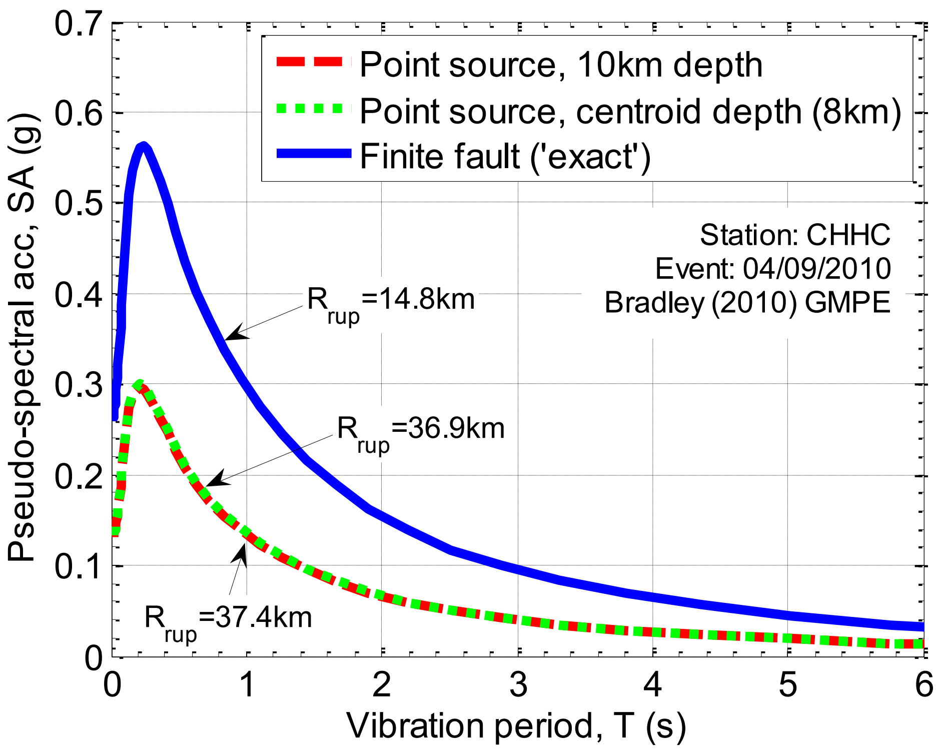

Figure 4: Effect of minimum earthquake depth of 10km and point source approximation in seismicity modelling on median response spectral amplitudes predicted at Christchurch hospital (CHHC) during: (a) 22 February 2011; and (b) 4 September 2010 earthquakes. The 'Finite fault' prediction is the correct prediction in terms of consistency between seismicity and ground motion modelling.

In order to emphasise the difference between the predicted response spectra in Figure 4, Figure 5 illustrates the ratio of response spectral amplitudes of the two approximations compared to the correct approach. It can be seen that generally the under-prediction increases with vibration period, with the point source approximations leading response spectral amplitudes which are up to 60% less (i.e. a ratio of 0.4) than that obtained using the consistent (i.e. finite fault) approach. Hence, clearly the current considerations of a minimum depth of 10km and point source approximation for background seismicity results in a significant under-prediction of the expected ground motions. For regions in which background seismicity provides a signficant contribution to the seismic hazard, such as Christchurch, the aforementioned approximations are likely to also result in a significant under-prediction of PSHA results, such as those that underpin NZS1170.5:2004.

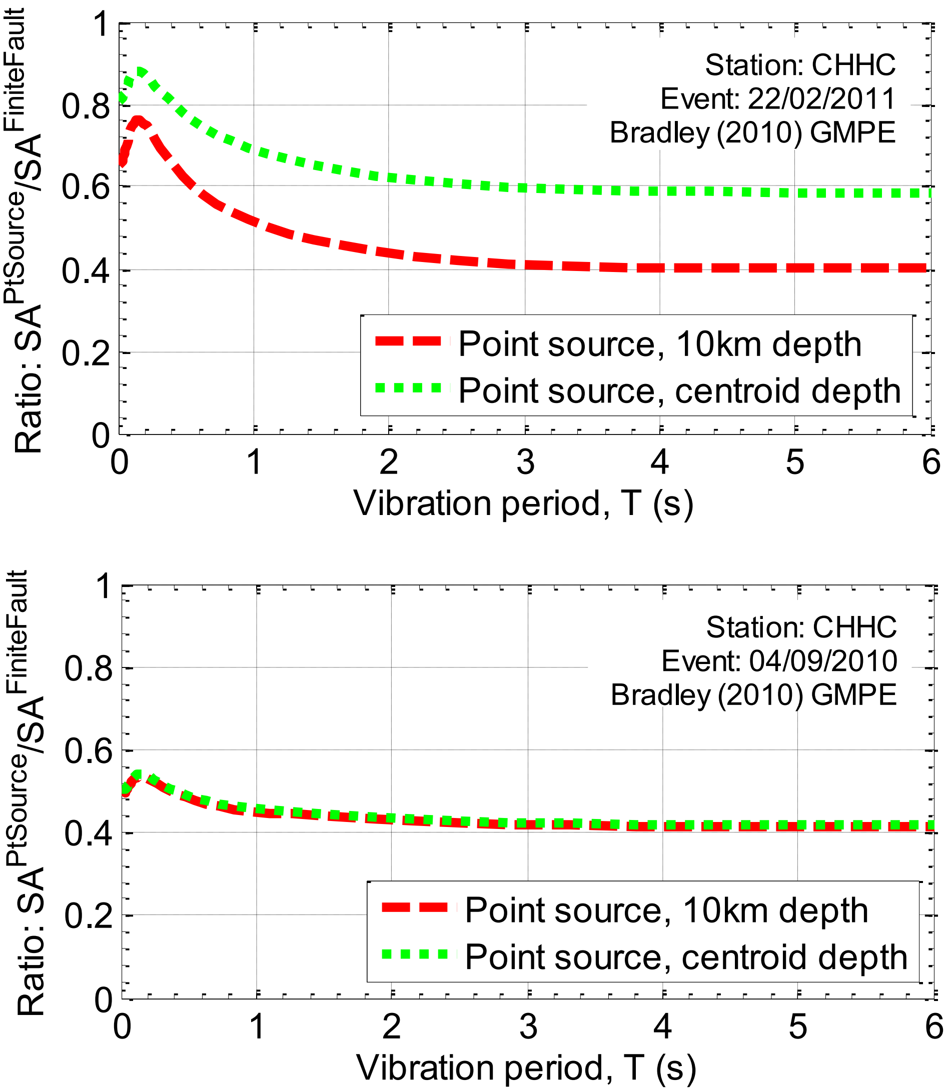

Figure 5: Ratio of response spectrum amplitudes predicted using the assumption of a minimum depth of 10km and/or point source approximation as given in Figure 5: (a) 22 February 2011; and (b) 4 September 2010 earthquakes.

3.2. Recommended Modifications in Seismicity Modelling

A summary of the salient discussion in this section and recommendations are:

- The Canterbury earthquake sequence occurred on faults which were not mapped, and therefore not specified in the fault-based component of New Zealand seismicity models. The occurrence of earthquakes other than those on known fault is however allowed for using 'background' seismicity. While the magnitude of the Darfield earthquake ($M_w 7.1$) is larger than the maximum magnitude of background seismicity allowed for by the seismicity underpinning NZS1170.5:2004, the most up-to-date seismicity model [5] allows for background events of up to $M_w 7.2$. The use of reverse-mechanism background seismicity in New Zealand seismicity models is specified conservatively since events with reverse-mechanism tend to systematically produce larger ground motions (as quantified by ground motion prediction equations).
- The Canterbury earthquakes occurred at centroid depths shallower than those allowed for in New Zealand seismicity models, and the models should therefore be updated to allow for such shallow events.
- In present New Zealand seismicity models, background seismicity is treated as point-sources. In contrast, ground motion prediction equations are based on finite-fault source-to-site distances. As source-to-site distances are always less than point-source distances, then this point-source representation results in an underestimation of seismic hazard (particularly for locations in the near-source region of the considered causative fault), and should be addressed in future seismic hazard analyses that use seismicity models with background seismicity.

4. Strong Ground Motions Observed in the Canterbury Earthquakes

Ground motion prediction equations (GMPEs) provide a probabilistic distribution of a ground motion intensity measure (e.g. SA at a given vibration period) for a given site location and earthquake scenario. As the GMPE provides a probabilistic prediction of ground motion intensity, then comparison with a single ground motion observation is insufficient to assess the performance of the GMPE. However, if it is shown (based on numerous observations) that a GMPE is unbiased and has the correct precision (i.e. the uncertainty is not too large or small) then comparison of the prediction from a GMPE and the observation can be used to identify any 'outlying' ground motions, and the physical reasons for the observations can be subsequently investigated.

The ground motions examined in this section are those resulting from the 4 September 2010 and 22 February 2011 earthquakes. The aim of this section is to examine the ground motions observed in these events with available GMPEs for use in New Zealand seismic hazard analysis. Based on these comparisons, several sub-sections are used to illustrate salient phenomena such as: near-source forward directivity; basin-generated surface waves; nonlinear response and liquefactions of surficial soil layers and vertical ground motions. The section begins by first emphasising GMPEs as a highly simplified empirical approach for ground motion, which are however parsimonious, and arguably the best approach at present for use in seismic hazard analyses used for engineering design.

4.1. Ground Motion Prediction Equation Preliminaries

4.1.1. The Simplicity of Ground Motion Prediction Equations (GMPEs)

It cannot be under-emphasised that the processes which lead to earthquake-induced ground motions exciting engineered structures are extremely complex. Even if one could predict the occurrence of earthquakes, the ground motions produced by an earthquake are a function of: (i) the location at which the earthquake starts (hypocentre); (ii) the manner in which the fault rupture propagates over the fault plane; (iii) the slip amplitude, direction (rake) duration (rise time), and stress drop at each location on the fault; (iv) the wave propagation path that seismic waves, generated by fault slip, take toward the site of interest; (v) the superposition of seismic waves, their reflection and amplification in travelling through different rock and soil mediums; and (vi) nonlinear effects of surficial soils (including the potential for liquefaction), among many others. All of the above phenomena are known to affect the characteristics (amplitude, frequency content, and duration) of ground motions.

Ground motion prediction equations do not seek to represent the complex physics which produce ground motions as described above. Instead ground motion prediction equations utilize ground motions that have been recorded in historical earthquakes, and develop a mathematical/statistical equation which can be used to predict (albeit with uncertainty) the severity of a ground motion intensity measure (e.g. SA at a given vibration period) given a particular site and earthquake scenario of interest. In order to further emphasise the simplicity of GMPEs it is useful to compare the particular variables of the site of interest and earthquake scenario that are used by such models, in comparison with the physical factors that influence ground motions as elaborated in the previous paragraph. In conventional GMPEs (such as those considered herein), details of the earthquake source are typically represented using only the earthquake moment magnitude, M_w, the faulting style (e.g. strike-slip, reverse, etc), and possibly the source depth (e.g. depth to the top of the fault plane). Comparison with points (i)-(iii) noted in the previous paragraph illustrates that such GMPEs do not consider the hypocentre location[1]; the time evolution of slip, and slip amplitude, stress drop, rise time and rake angle. Similarly, the effects of wave propagation in GMPEs are typically accounted for simply using the nearest distance from the earthquake source (finite-fault) to the site of interest, R_{rup}, and neglect the complex wave propagation path, including reflections, refractions, and superposition through heterogeneous medium (points (iv) and (v) above). Finally, while the surficial soil layers represent only 10's -100's of meters of the wave propagation path (in comparison to the typically 10's of kilometres through basement rocks from the source to site), the significant spatial variably of such soils over short distances means that 'local site effects' are known to have a profound influence on surface ground motions. Local site effects (particularly for strong ground motion) are a function of the stratigraphy of the site (i.e. the 'layering' of different geologic units), the mechanical and physical properties, and insitu state of the soils (all of which affect the stress-strain response, including hysteretic energy dissipation and nonlinearity). In contrast, it is typical that GMPEs represent soils by a simple alphabet-based soil classification. For example, in NZS1170.5:2004, local site conditions are considered in five distinct classes (A-E), which are A: Hard Rock; B: Rock; C: Shallow Soil; D: Deep or Soft Soil; and E: Very soft soil. Hence none of the aforementioned factors that affect local site effects are considered explicitly in a GMPE other than those implicitly used to determine the site classification (i.e. A-E) of the site. It should be noted that more recent GMPEs [7, 19] typically depart from such an alphabet-based site classification and instead use the average shear wave velocity of the top 30m of the site ($V_{s,30}$), and the depth to which the site materials attain some shear wave velocity (e.g. depth to $V_s = 1.0$km/s).

The above paragraph illustrated the simplicity of GMPEs relative to the physics causing earthquake-induced ground motions. As GMPEs are mathematical relationships fit to empirical data, then although such relationships are oversimplified, they provide an acceptable approximation for ground motion scenarios which are well represented by empirical data. However, as previously noted, there is a paucity of recorded strong motions from large magnitude earthquakes at close source-to-site distances, which are often the governing scenarios in the design of structures. Hence, when comparing ground motion observations with GMPEs, bearing all of the above simplifications in mind, it should be expected that individual ground motions will exhibit significant variability. However, a good GMPE should be unbiased when compared with a sufficient sample of data and have the correct precision (i.e. the uncertainty given by the prediction should be consistent with the variability in the observations).

As a final point, it is worth noting that physics-based models for ground motion prediction are a present research topic within the physical sciences and engineering seismology. While such models represent the physics of ground motion in a more precise manner than GMPEs, they require significantly more input information. At present it is the consensus of many (including the author), that such methods are insufficiently constrained to provide consistently reliable results for 'forward' prediction (as opposed to demonstrating capability based on comparison with observed events).

4.1.2. Scalar Ground Motion Amplitude for Bi-directional Motions: Larger or 'average' component?

The ground motion at a site of interest is comprised of six components: three translational components, and three rotational components. As rotational components are typically ignored, only the three translational components of ground motion are typically recorded. While vertical ground motions are not unimportant (see section 4.3.4), for earthquake-induced ground motion the horizontal translational components are principally those most damaging to structures. As previously discussed, in engineering it is common to represent ground motion in terms of a

[1] Hypocentre location is however considered in models that adjust conventional GMPEs for near-source forward directivity effects [e.g. 18]

response spectrum plot. Such response spectra are defined for a single component of ground motion. Therefore, it is desired to have a scalar quantity of spectral acceleration which can be used to represent the bi-directional ground motion. Several options for achieving this are discussed below, particularly those relating to NZS1170.5:2004 and international best-practice.

Since horizontal ground motions contain two orthogonal components, then ground motion intensity measures can be computed separately for each component. Figure 6 illustrates the two 'as-recorded' components of ground motion at the Christchurch Cathedral College (CCCC) station resulting from the 22 February 2011 earthquake. It can be seen that there are differences in the character of the ground motion in these two orthogonal directions, for example, the peak ground acceleration is 0.49g for component 1 and 0.38g for component 2.

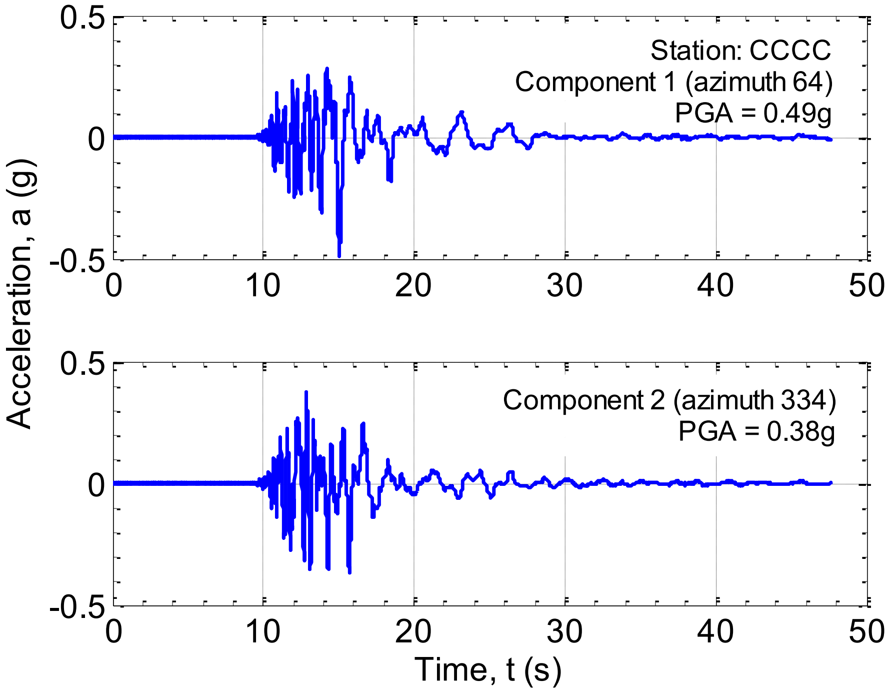

Figure 6: Acceleration histories of the ground motion recorded at Christchurch Cathedral College (CCCC) station during the 22 February 2011 earthquake: (a) component 1 oriented at an azimuth of 64 (i.e. 64 degrees east of north); and (b) component 2 oriented at an azimuth of 334.

There are two conventional approaches for obtaining a single ground motion intensity measure from bi-directional horizontal ground motions. The first approach is to take the intensity measures in the two orthogonal directions and select the maximum. For the case where SA is the intensity measure (for which PGA=SA(T=0)), this can be written as:

$$SA^{Larger} = \max\,(SA_1, SA_2) \tag{5}$$

where SA_1 and SA_2 are the values of spectral acceleration for the two orthogonal components. Thus for the example in Figure 6 discussed above:

$$PGA^{Larger} = \max(0.49g, 0.38g) = 0.49g \tag{6}$$

The second approach it to determine an 'average' of the two orthogonal components. As spectral accelerations are well represented by a lognormal distribution, as utilized in GMPEs, then the 'average' of the two components is considered with respect to the logarithms of spectral acceleration, that is:

$$log(SA^{GeoMean}) = \frac{log(SA_1) + log(SA_2)}{2} \tag{7}$$

Using logarithm rules, the above expression is equivalent to:

$$SA^{GeoMean} = \sqrt{SA_1 * SA_2} \tag{8}$$

where $SA^{geomean}$ is referred to as the 'geometric mean' (as opposed to an arithmetic mean). Thus for the example in Figure 6 discussed above:

$$PGA^{GeoMean} = \sqrt{0.49g * 0.38g} = 0.43g \tag{9}$$

By definition, SA^{Larger} will always be greater than $SA^{GeoMean}$. Furthermore, because $SA^{GeoMean}$ represents the 'average' of the two components of ground motion, then it is a more 'stable' measure of ground motion intensity, as will be demonstrated below.

Both $SA^{GeoMean}$ and SA^{Larger} are based on the use of SA values of the ground motion components in their 'as-recorded' orientations. These 'as-recorded' orientations are arbitrary and do not represent any orientations in particular, such that the two primary axes of a building. Using a rotation matrix it is trivial to rotate the two orthogonal ground motion components to obtain the ground motion in any arbitrary orientation. Figure 7 illustrates the effect of rotating the orientation of the two components of ground motion on the values of the peak ground acceleration (only the non-redundant 90degrees of rotation are shown), as well as annotating the as-recorded values. It can be seen, for example, that the component 1 ground motion PGA value varies from approximately 0.37 to 0.43g, and that component 2 varies from 0.4g to 0.49g. Figure 7 also illustrates that PGA^{Larger} varies between 0.4-0.49g (i.e. a range of 20%), while $PGA^{GeoMean}$ varies from 0.395-0.445g (i.e. a range of 12%). As a result of these axis rotation effects, Boore et al. [20] recommended the use of orientation-independent ground motion intensity measures, such as $SA^{GeoMean(50^{th})}$ which is the 50^{th} percentile of the $SA^{GeoMean}$ values over all the non-redundant rotation angles (as shown in Figure 7). Beyer and Bommer [21] illustrated that from a practical point-of-view, the smaller variability of $SA^{GeoMean}$ on rotation angle means that $SA^{GeoMean}$ can be considered as equal to $SA^{GeoMean(50^{th})}$ if a sufficient number of ground motions are considered (e.g. Figure 7 illustrates the error is at most 8% for a single ground motion, and as the errors are random for different records they will converge quickly to an insignificant level).

NZS1170.5:2004 is based on the seismic hazard analysis models given in Stirling et al. [6]. This seismic hazard analysis uses the 'larger component' definition of the McVerry et al. [22] GMPE, and hence it may be considered that the results of NZS1170.5:2004 are representative of the larger component. However, it must be remembered that the 'larger component' definition is not the absolute largest value using any orientation, but the larger of the two values in their as-recorded orientation. In the case of Figure 7 above it can be seen that the largest component in the as-recorded orientation is close to the maximum value of PGA in any orientation, however this is not generally the case. For example, in the case of the Canterbury Botanic Gardens (CBGS) ground motion resulting from the 22 February 2011 earthquake, as illustrated in Figure 8, the value of the 'larger component' is approximately 0.57g, however the actual maximum PGA value in any direction is approximately 0.7g.

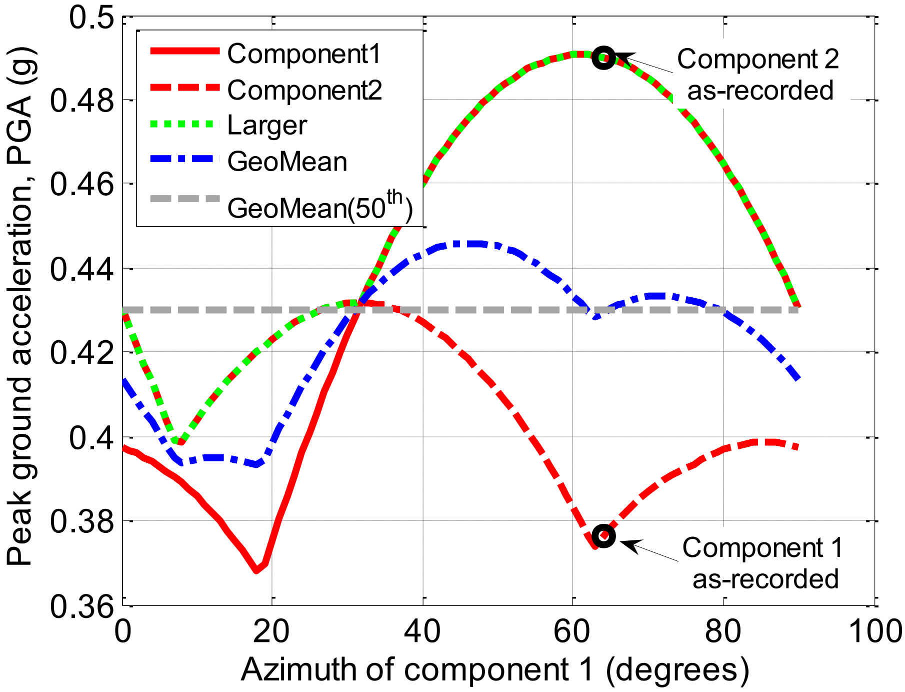

Figure 7: Effect of changing the orientation of recording instruments on the values of peak ground acceleration obtained for the CCCC ground motions in Figure 6.

Given that the 'larger component' is dependent on the orientation of the ground motion instrument then it does not ensure that the value will in fact be the maximum value that occurs in any orientation. One option to add conceptual robustness would be to consider this peak value in any orientation. However, from a structural-response perspective this is highly conservative given that structures tend to vibrate along specific axes. Stewart et al. [23] provide an elaborate discussion of the reasons why the maximum value in any orientation is a poor choice, and why the geometric mean is preferred.

Hence in the comparisons to following of ground motion observations from the Canterbury earthquakes preference is given to representation of bi-directional ground motions using the geometric mean of the two components. Because NZS1170.5:2004 may be regarded as based on the ill-defined 'larger-component' then plots which compare observations with the NZS1170.5:2004 design response spectra show the ground motions in two orthogonal axes, as well as their geometric mean. It is recommended that future seismic hazard analyses in New Zealand utilize GMPEs for the geometric mean (or geometric mean 50th percentile), rather than this ill-defined larger component.

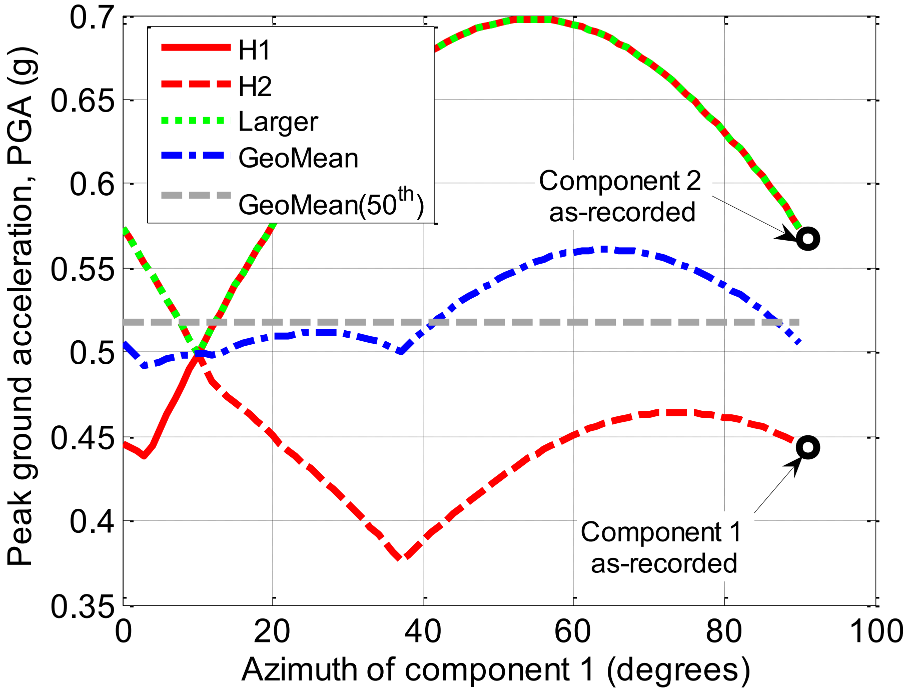

Figure 8: Effect of changing the orientation of recording instruments on the values of peak ground acceleration obtained for the CBGS ground motion from the 22 February 2011 earthquake.

4.2. Comparison of Observed Ground Motion Response Spectra with Empirical Prediction Models for Horizontal Ground Motion

In this section response spectral amplitudes of ground motions from the 4 September 2010 and 22 February 2011 are compared with NZ-specific GMPEs that are presently available for use in seismic hazard analysis for locations in New Zealand. Recent nationwide seismic hazard analyses for New Zealand [5, 6, 16], in particular those underpinning NZS1170.5:2004, use the McVerry et al. [22] GMPE. The McVerry et al. GMPE can be used to predict either the 'larger' or 'geometric mean' of two ground motion components. For reasons elaborated in section 4.1.2, the geometric mean prediction of the McVerry et al. model will be compared with the geometric mean's of the observed ground motions.

While the McVerry et al. model was published in the public domain in 2006, it was developed much earlier, being completed in 1997 and first published (but without equations and coefficients) as a conference paper in 2000 [24]. The model is based on '1997-version' GMPEs developed for California [25] and general Subduction Zones [26]. The McVerry et al. model used an empirical database comprising a total of 49 earthquakes and 435 records from New Zealand in the period 1966-1995. An additional 66 records from 17 foreign crustal events were also added to constrain the active shallow crustal model where NZ data were deemed insufficient.

As a result of the GeoNet project, there are presently more than 3000 strong ground motion records recorded from earthquakes in New Zealand. Due to the significant increase in strong motion data, and the fact that the revised Next Generation Attenuation GMPEs in California (published in 2008 [27]) are considered as significant improvements over the '1997-version' GMPEs, Bradley [7] developed a NZ-specific active shallow crustal GMPE (using 2852 ground motions) based on the Chiou et al. [19] GMPE for California, with modifications for NZ-specific features. Hence both the McVerry et al. and Bradley GMPEs will be considered with respect to the observed ground motions from the Canterbury earthquakes. For brevity, these two different models will be referred to as B10 and McV06, respectively.

4.2.1. Response Spectral Amplitudes from the 22 February 2011 Christchurch Earthquake

Figure 9 and Figure 10 illustrate the amplitudes of response spectral ordinates observed in the 22 February 2011 Christchurch earthquake compared to the predictions of the B10 and McV06 GMPEs, respectively. The prediction of the empirical models is shown for the median (i.e. 50th percentile), as well as the 16th and 84th percentiles. The results are shown for four vibration periods of 0.0, 0.2, 1.0 and 3.0 seconds, which span a range of vibration periods that are of interest for structural response. Each plot shows the response spectral amplitudes as a function of the nearest distance from the earthquake source (i.e. finite-fault) to the site at which the ground motion was recorded, R_{rup}; and data are also coloured according to the NZS1170.5:2004 site class of each instrument location. Four letter codes represent names of the ground motion locations, which are referred to subsequently. Ground motion data beyond R_{rup} = 50km are not shown as their amplitudes are small enough to not be of concern for engineered structures. In addition to the visual comparison between observations and prediction, mixed-effects regression [28, 29] was utilized in order to determine the inter- and intra-event results for each vibration period. The value of the normalized inter-event residual (η) is also shown in the inset of each figure, and can be considered as a measure of the overall bias of the model for all recorded ground motions (within 50km in this case), and for the particular spectral ordinate considered. A value of $\eta = 0$ indicates no bias, while a value of $\eta = 1.0$, for example, indicates that the observations are, on average, one standard deviation above the median prediction.

The results of Figure 9 illustrate that the B10 GMPE is able to capture the source-to-site distance dependence of the observations with good accuracy (i.e. low bias) and precision (i.e. correct variability). The inter-event term, η, indicates that the model has very small bias for vibration periods of T=0.0, 0.2 and 1.0s (i.e. η=-0.217, -0.28, and 0.106, respectively), but that there is a notable under-prediction of SA(3s) amplitudes for distances less than 10km (i.e. η=0.907). The potential reasons for the under-prediction of long-period ground motions at these short source-to-site distances are primarily attributed to near-source directivity, basin-generated surface waves, and nonlinear response of surficial soils, and are elaborated upon subsequently.

The results of Figure 10a illustrate that the McV06 model generally provides a good prediction of the observed PGA's within 50km, although there is a slight over-prediction ($\eta = 0.499$), particularly for distances beyond 25km. Figure 10b illustrates that the prediction of SA(0.2s) of the McV06 model is significantly above the average of the observations for all source-to-site distances ($\eta = -1.513$). Figure 10c illustrates that the McV06 model incorrectly models the variation in SA(1s) amplitudes as a function of source-to-site distance, with the observed amplitudes attenuating with distance notably faster than that predicted by the McV06 model. Because of the under-prediction of the model for short distances, and over-prediction for larger distances, the small value of $\eta = -0.106$ is obtained for SA(1s). Figure 10d illustrates that the McV06 significantly under-predicts the SA(3s) amplitudes that were observed ($\eta = 2.102$).

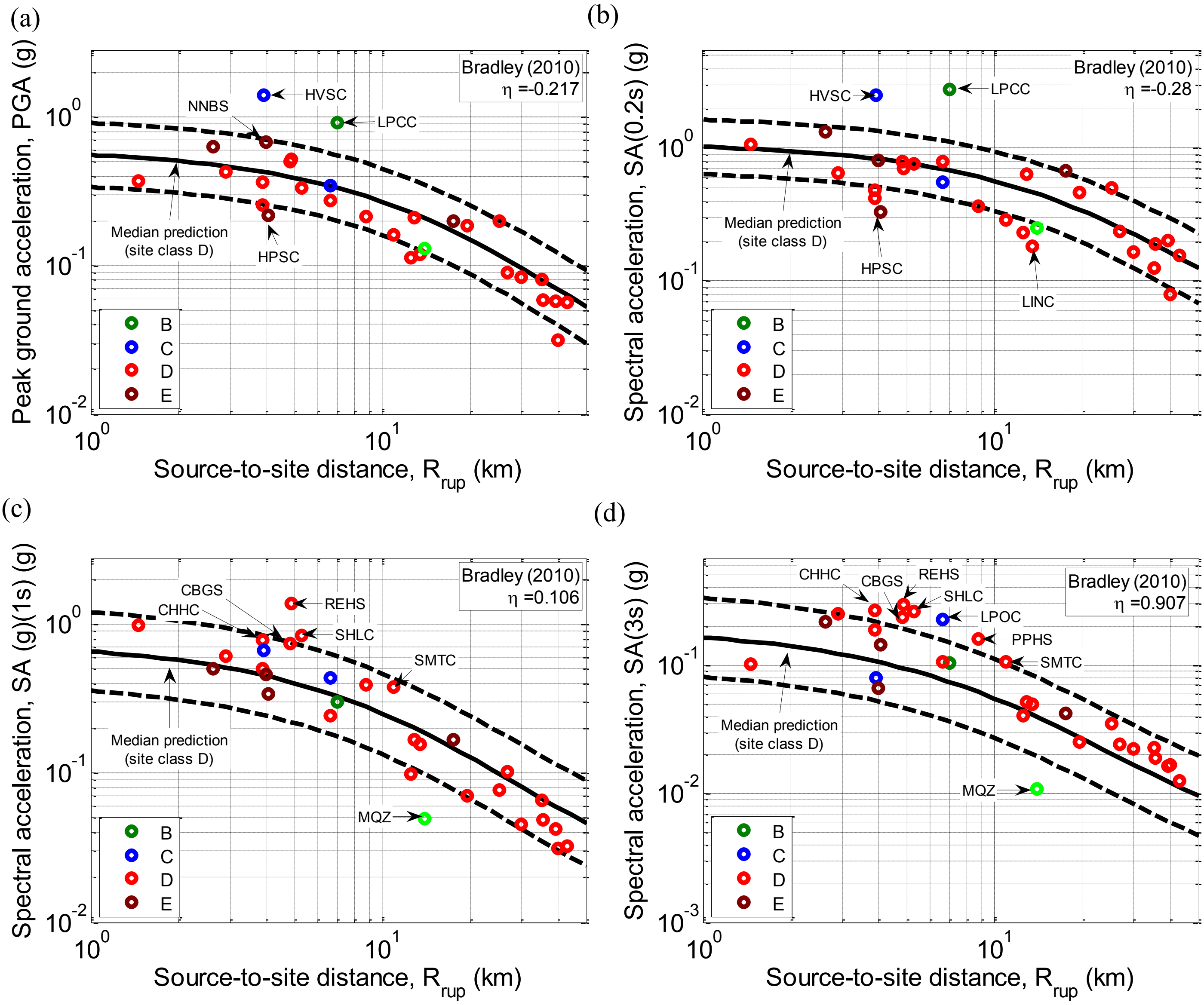

Figure 9: Comparison of observed spectral accelerations (periods 0.0, 0.2, 1.0, and 3.0) from the 22 February 2011 Christchurch earthquake with the Bradley [7] GMPE for site class D soil conditions (median given by the solid line and 16th and 84th percentiles by dashed lines).

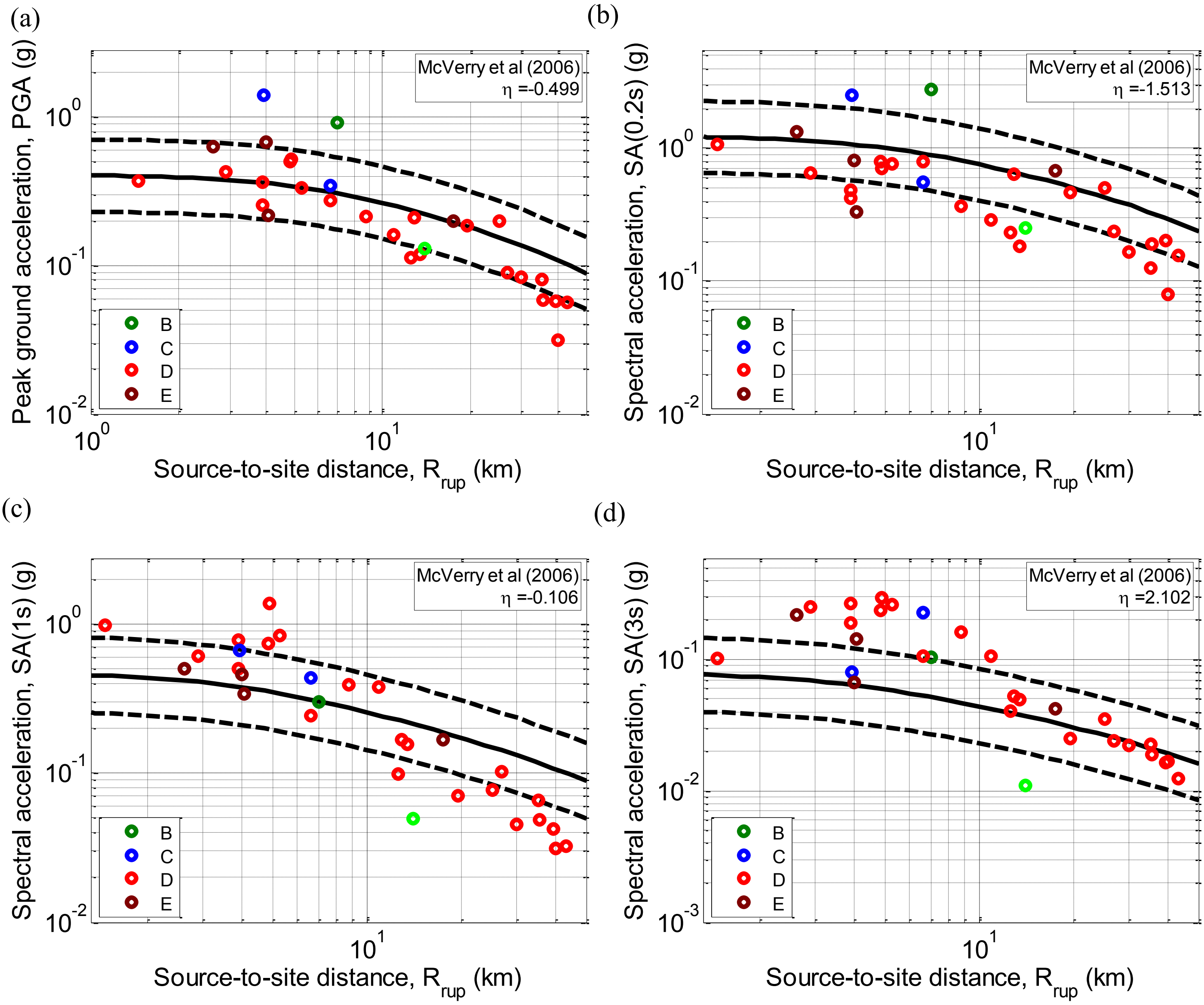

Figure 10: Comparison of observed spectral accelerations (periods 0.0, 0.2, 1.0, and 3.0) from the 22 February 2011 Christchurch earthquake with the McVerry et al. [22] GMPE for site class D soil conditions (median given by the solid line and 16th and 84th percentiles by dashed lines).

In order to clearly illustrate the results of Figure 9 and Figure 10, Figure 11 provides a comparison of the response spectra of the ground motion observed at Christchurch Hospital (CHHC) resulting from the 22 February 2011 earthquake. The observed response spectra are presented for the north and east components of the ground motion, as well as the geometric mean response spectra, and model predictions (also for the geometric mean). It can be seen that while the model predictions are a relatively smooth function of vibration period, the observed response spectra vary more erratically with vibration period. Figure 11a illustrates that, over all vibration periods the B10 model provides a good prediction of the observed ground motion response spectra with the observed geometric mean being close to that of the median prediction. In contrast, Figure 11b illustrates that the McV06 model significantly over-predicts the short period response spectra at around T=0.2s (i.e. as illustrated in Figure 10b), and that the McV06 model significantly under-predicts the ground motion for longer vibration periods (i.e. as illustrated in Figure 10c at close distances and Figure 10d).

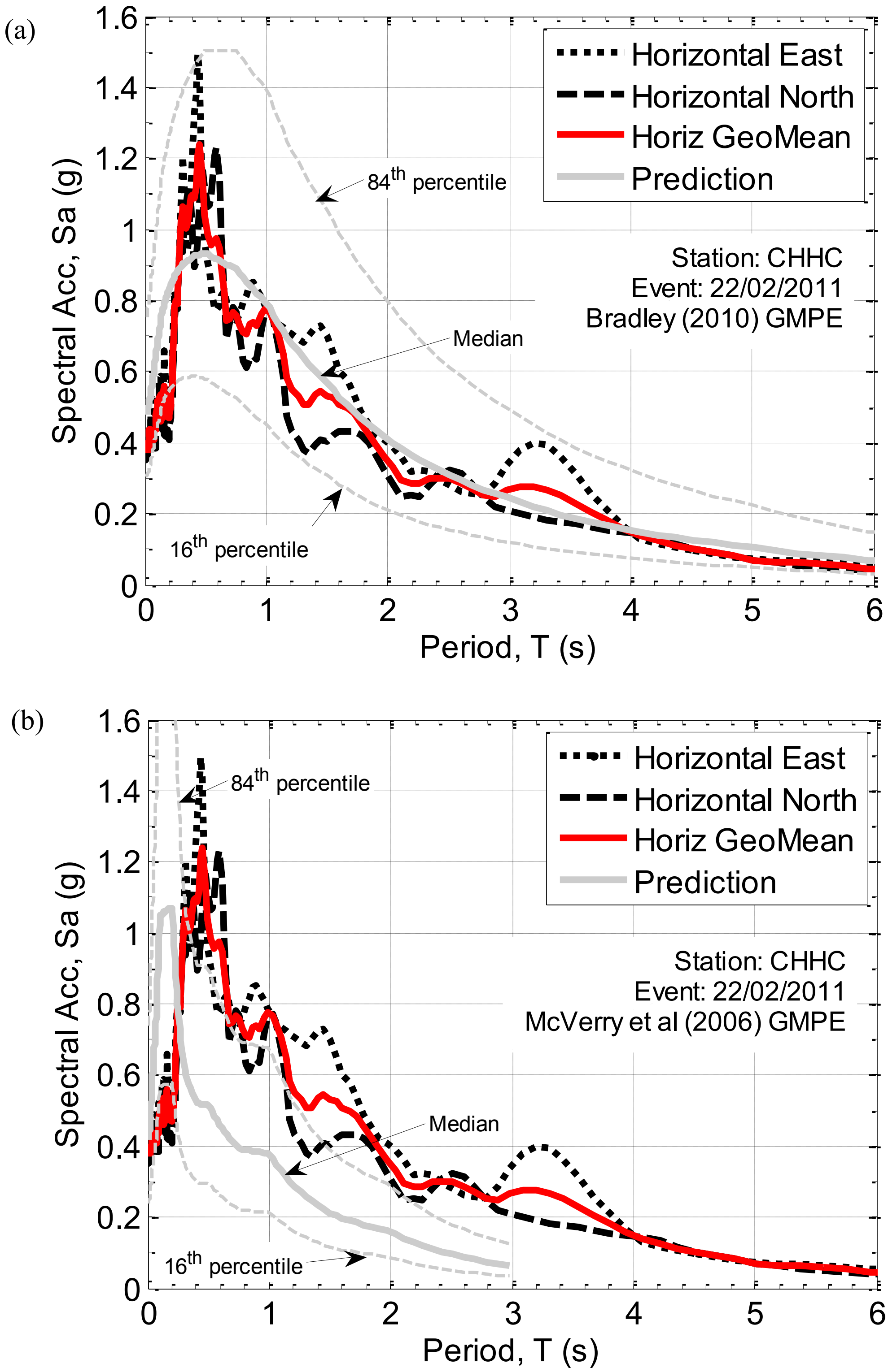

Figure 11: Comparison of the pseudo-acceleration response spectra (SA) observed at Christchurch Hospital (CHHC) during the 22 February 2011 Christchurch earthquake (both North and East components, and the geometric mean) with the empirical prediction based on the NZ-specific: (a) Bradley [7] model; and (b) McVerry et al. [22] model. Note that the McVerry et al. model provides predictions for T≤3s only.

4.2.2. *Response Spectral Amplitudes from the 4 September 2010 Darfield Earthquake*

Figure 12 and Figure 13 compare the observed response spectral amplitudes of ground motions from the 4 September 2010 earthquake. The notational convention in Figure 12 and Figure 13 is the same as that in Figure 9 and Figure 10, which presented results for the 22 February 2011 earthquake. Because of the larger magnitude of the 4 September 2010 earthquake (M_w7.1) ground motion response spectral amplitudes recorded within 100km are shown in Figure 12 and Figure 13, which can be considered of significance to engineered structures (in contrast with 50km considered for the 22 February 2011 M_w6.3 earthquake).

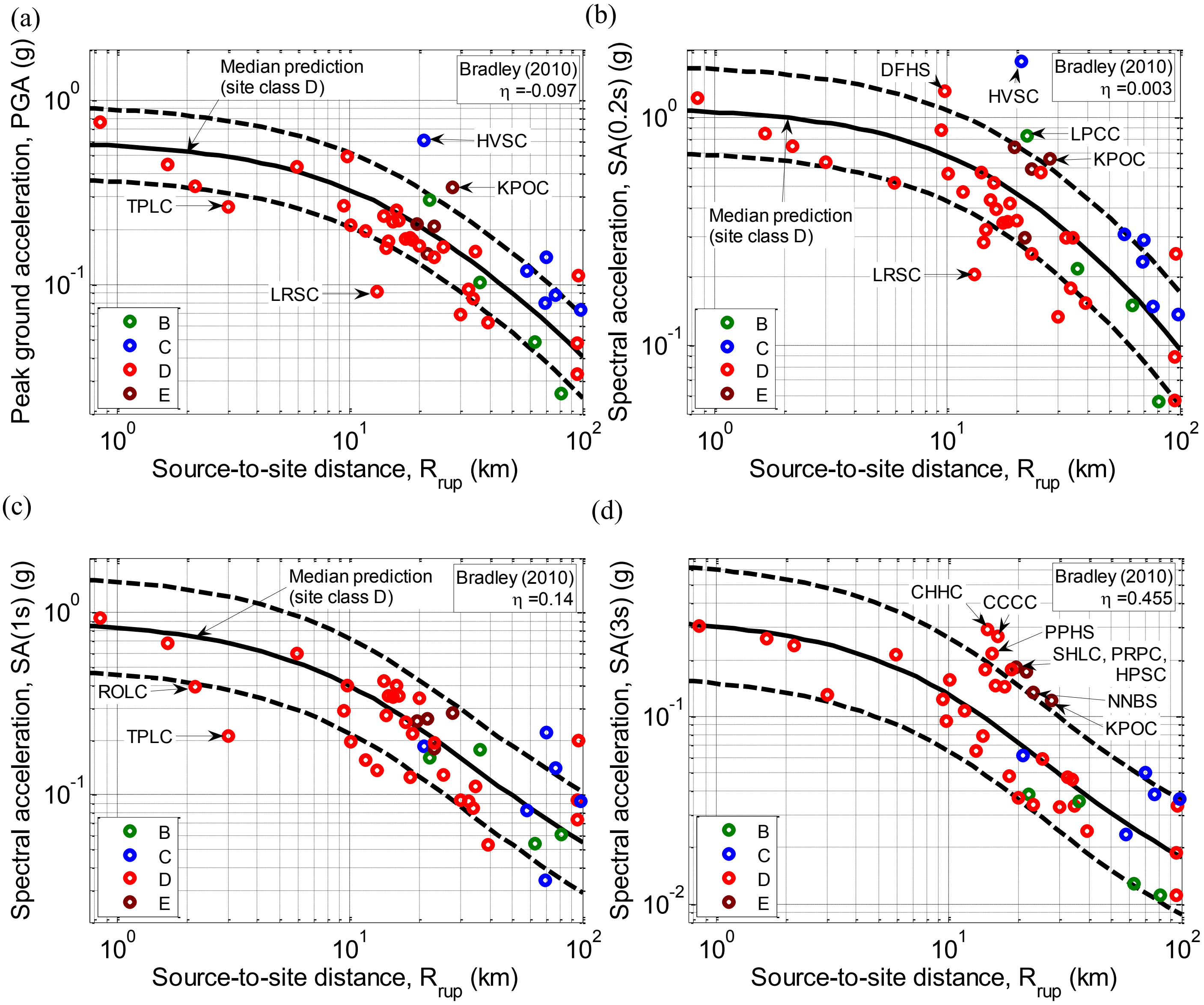

Figure 12: Comparison of observed spectral accelerations (periods 0.0, 0.2, 1.0, and 3.0) from the 4 September 2010 Darfield earthquake with the Bradley [7] GMPE for site class D soil conditions.

Figure 12 illustrates that the B10 GMPE provides an accurate and precise prediction of short and moderate period spectral amplitudes, with inter-event terms (i.e. bias) of η = -0.097, 0.003, and 0.14. Spectral amplitudes for a vibration period of 3 seconds, representative of longer period ground motion intensity, are more significantly under-predicted by the B10 GMPE, particularly at source-to-site distances of 10-30km, as a result of near-source forward directivity (elaborated upon subsequently).

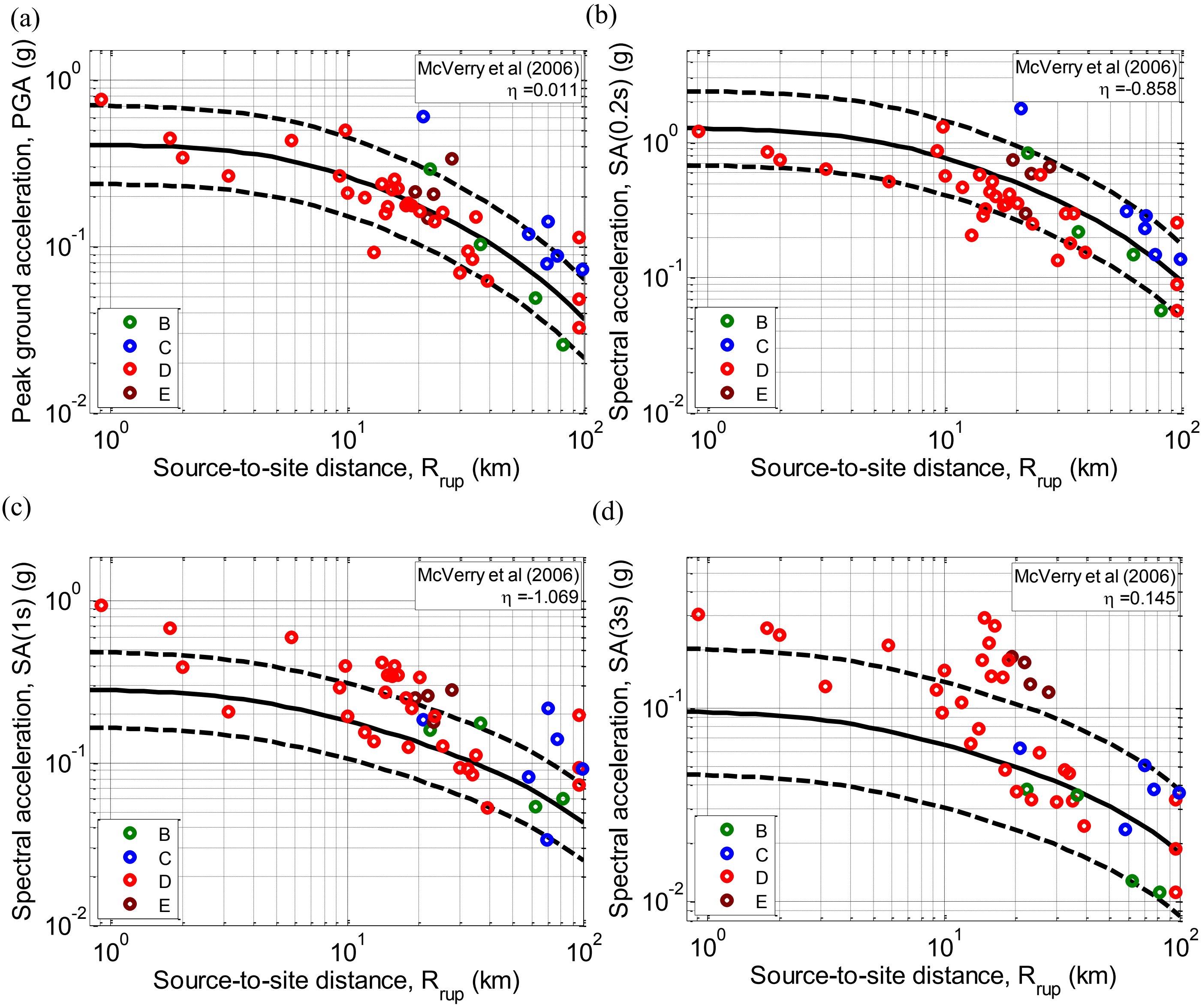

Figure 13: Comparison of observed spectral accelerations (periods 0.0, 0.2, 1.0, and 3.0) from the 4 September 2010 Darfield earthquake with the McVerry et al. [22] GMPE for site class D soil conditions.

Figure 13 illustrates that, similar to the comparisons of the McV06 model and the observed ground motions from the 22 February 2011 earthquake, the McV06 model provides an accurate prediction of PGA (i.e. Figure 13a, $\eta = 0.011$); a notable over-prediction of SA(0.2s) (i.e. Figure 13b, $\eta = -0.858$); and significant under-predictions of long-period ground motion intensities at short source-to-site distances (i.e. SA(1s) and SA(3s) in Figure 13c and Figure 13d, respectively).

Figure 14 compares the ground motion spectral amplitudes recorded at Christchurch Hospital (CHHC) during the 4 September 2010 earthquake with the predictions of the B10 and McV06 models. For the CHHC case, in particular, it can be seen that apart from the high SA(0.2s) amplitudes predicted by the McV06 model, the two predictions are similar for this particular ground motion. Both ground motion prediction equations do not capture the large increase in response spectral amplitudes in the North-South (approximately fault-normal) component of ground motion that results from forward-directivity effects (discussed in section 4.3.1).

The ground motion intensity at Christchurch Hospital during the 4 September 2010 earthquake was smaller (at high and moderate frequencies) than that during the 22 February 2011 earthquake as a result of the larger source-to-site distance in the former event. In order to illustrate the two models performance for a location closer to the causative faults of the 4 September 2010 earthquake, Figure 15 illustrates the observed ground motion at Greendale relative to the B10 and McV06 model predictions. The Greendale ground motion record (GDLC) was obtained from an instrument located near the surface rupture of the Greendale fault ($R_{rup} = 0.3km$). Figure 15a illustrates that the ground motion response spectral amplitudes are well predicted by the B10 GMPE, with the geometric mean of the GDLC observation close to the median prediction. In contrast, Figure 15b illustrates that the prediction of the McV06 GMPE: (i) contains a large peak at approximately SA(0.2s); and (ii) provides a significant under-prediction for moderate and long vibration periods (similar to Figure 11b for the 22 February 2011 earthquake). Hence, it can be stated that the McV06 GMPE generally provides a poor prediction of ground motions with small source-to-site distances, i.e. locations close to faults, which have the largest ground motion intensities, and therefore are of primary concern from a structural design viewpoint.

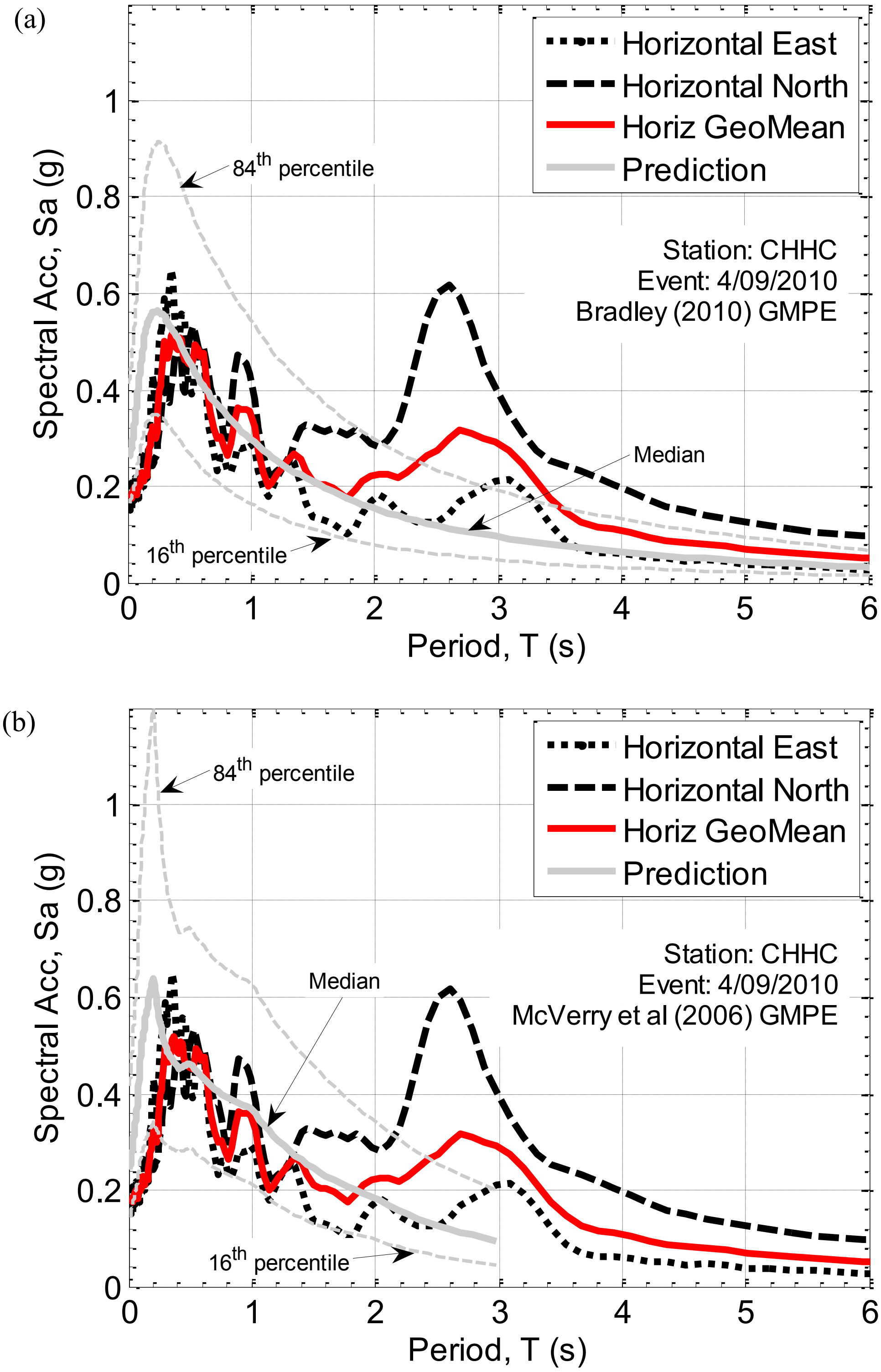

Figure 14: Comparison of the pseudo-acceleration response spectra (SA) observed at Christchurch Hospital (CHHC) during the 4 September 2010 earthquake (both North and East components, and the geometric mean) with the empirical prediction based on the NZ-specific: (a) Bradley [7] model; and (b) McVerry et al. [22] model. Note that the McVerry et al. model provides predictions for T≤3s only.

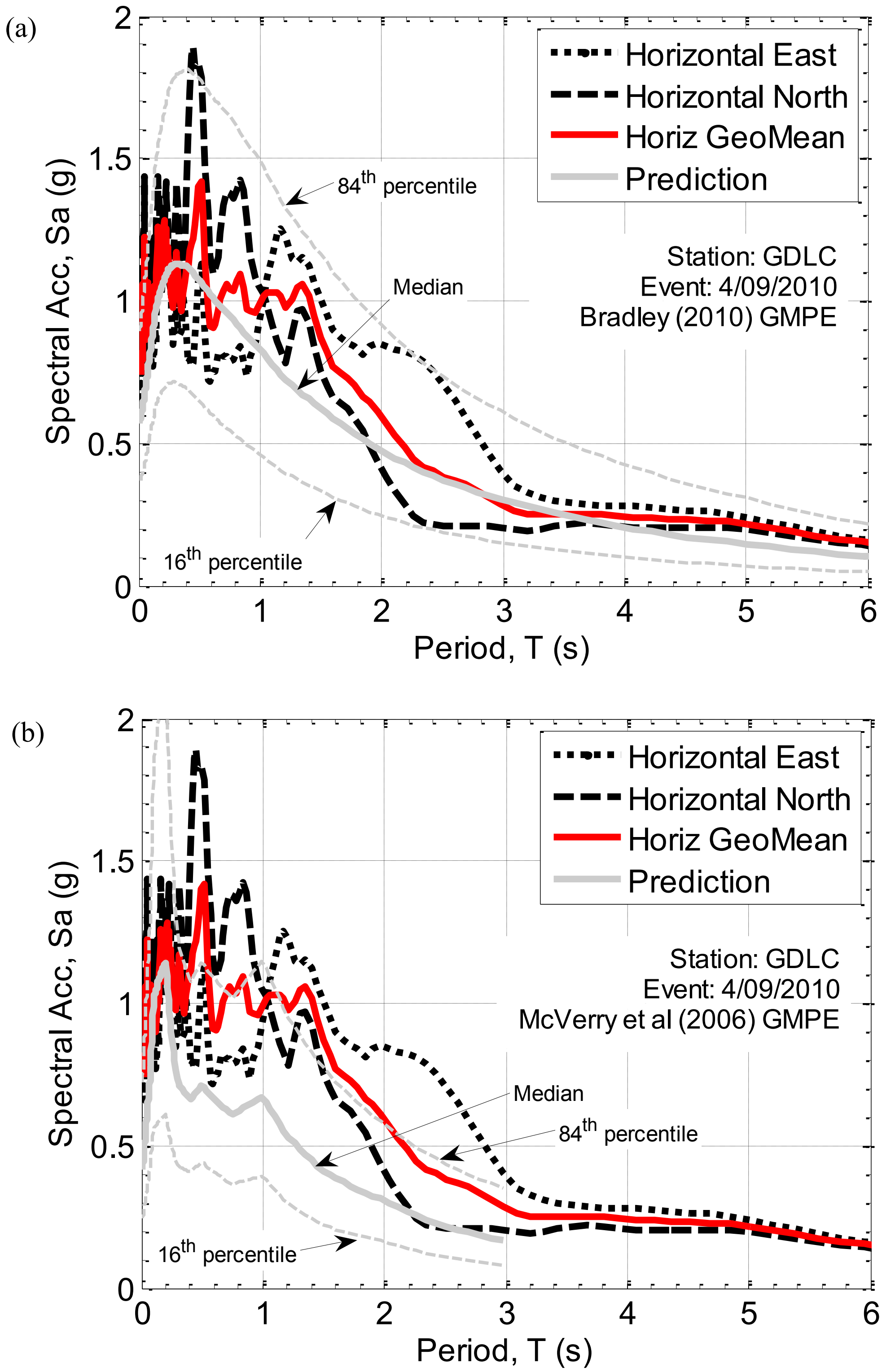

Figure 15: Comparison of the pseudo-acceleration response spectra (SA) observed at Greendale (GDLC) during the 4 September 2010 earthquake (both North and East components, and the geometric mean) with the empirical prediction based on the NZ-specific: (a) Bradley [7] model; and (b) McVerry et al. [22] model. Note that the McVerry et al. model provides predictions for T≤3s only.

4.2.3. Summary of Comparisons Between Observations and Empirical GMPEs

The previous two sections have illustrated that, in general, the ground motions from the 22 February 2011 and 4 September 2010 earthquakes are consistent with the Bradley [7] model, which is a New Zealand – specific version of the Chiou et al. [19] model for California, and consistent with the state of the art in ground motion prediction equations at present. In contrast, the McVerry et al. [22] model, which is used in the majority of New Zealand seismic hazard analyses, in particular those underpinning NZS1170.5:2004, provides a poor prediction of spectral amplitudes, other than PGA, particularly at small source-to-site distances.

Among other things, Webb et al. [30] state that the Canterbury earthquakes have higher energy magnitudes than moment magnitudes, and therefore that the Canterbury earthquakes have above average ground motions, and above average stress drop. The ground motion comparison in Figure 3.10 of Webb et al. [30] compares the observed ground motion SA(1s) values with those predicted using the McV06 GMPE (i.e. the same as Figure 10c but using the 'larger component' as opposed to the 'geometric mean' as used herein (see section 4.1.2 as to why geometric mean is used)). Webb et al. [30] subsequently investigate the use of a modification factor to the McV06 GMPE to account for an implied high stress drop. From a theoretical point-of-view, a higher than average stress drop should be most apparent for high frequency ground motion (e.g. PGA and SA(0.2s)), and affect the amplitude of ground motions at all source-to-site distances. Comparison of the results in Figure 9 and Figure 12 illustrate that the high-frequency ground motion intensities of recordings from both the 22 February 2011 and 4 September 2010 earthquake are consistent with the B10 GMPE. Comparison of Figure 10a and Figure 13a also illustrates that the PGA observations are also consistent with the McV06 GMPE. Hence, comparison of the SA(1s) observations and the McV06 prediction in Figure 10c and the B10 prediction in Figure 9c illustrates that the departure of the McV06 prediction from the observations is simply a result of the inability of the McV06 model to correctly predict the variation in SA(1s) amplitudes as a function of source-to-site distance. This assertion is further reinforced by examination of Figure 3.11 of Webb et al. which illustrates that adjustment factors for an implied high stress drop provide a minor increase in spectral amplitudes at all source-to-site distances, but do not change the variation in amplitudes with source-to-site distance. It is also noted that Abrahamson [31] argues that empirical evidence does not suggest that ground motions from these have abnormally high stress drop, and that earthquake stress drops bear no empirical correlation with the level of seismic activity of the causative region, and also that Archuleta [32] notes that energy magnitude is highly uncertain, and not directly related to stress drop.

As discussed in section 4.1, it must be remembered that GMPEs represent a highly simplified empirical representation of the physics that affect the characteristics of ground motions and therefore they are only robust for the prediction of ground motion scenarios which are well represented within the empirical database of ground motions upon which a given GMPEs is developed. Because of the large number of strong ground motions, that were fortunately recorded due to a well developed and maintained strong motion instrumentation network, there are several salient phenomena present in the ground motions previously summarised that warrant a critical examination. Subsequent sections are devoted to demonstrating evidence of these phenomena and discussing the consequent implications of such observations relative to existing predictive models and the NZS1170.5:2004 design standard.

4.3. Salient Physical Phenomena in Observed Ground Motions and Implications

Figure 9 and Figure 12 annotated various strong motion stations which lie outside the 16th and 84th percentiles of the Bradley [7] empirical prediction. As was noted previously, because of the simplicity of GMPEs, it should not be unexpected that ground motions deviate from the median

GMPE prediction, however significant departures (i.e. below the 16th or above the 84th percentiles) are indicative of the predominance of physical phenomena which are not well represented in the empirical model (or its underling empirical database of historically recorded ground motions). The purpose of the following sub-sections is to utilize the observed strong ground motions in the 22 February 2011 and 4 September 2010 earthquakes to illustrate phenomena which are not well accounted for in empirical GMPEs, which typically are utilized in seismic hazard analysis and form the basis for seismic design standards, e.g. NZS1170.5:2004, and the subsequent implications for such GMPEs and seismic design standards.

4.3.1. Near-source Forward Directivity Effects

Forward directivity is a phenomenon which occurs in the near-source region resulting from the alignment of the rupture front, direction of slip, and the source-to-site direction. The manifestation of forward directivity is the arrival of a large portion of the radiated seismic energy in a single pulse at the beginning of the ground motion record oriented in the direction normal to the fault strike, and has a particularly large damage potential due to its large amplitude and short duration. Forward-directivity effects occur in the near source region in earthquakes of all magnitudes [33], and their significance, from an engineering perspective, increases with increasing earthquake magnitude (due to a larger rupture duration). It must be stressed that forward directivity effects do not occur in all directions from a fault in the near-source region. If the direction of rupture propagation is 'away' from the site of interest then backward directivity effects occur, which will result in longer duration ground motion, but of a lower amplitude [34]. As will be illustrated below, forward directivity effects were signficant for the 4 September 2010 Darfield earthquake as a result of its size ($M_w 7.1$), strike-slip faulting mechanism and rupture propagation of the central and eastern section of the Greendale fault toward Christchurch [35]. In contrast, forward directivity effects from the 22 February 2011 Christchurch earthquake are less significant, relative to the Darfield earthquake as a result of its size ($M_w 6.3$), and also are prevalent only in a smaller area in the eastern suburbs of Christchurch as a result of the mis-alignment between the direction of slip on the fault and the inferred direction of rupture propagation on the fault [36-38].

As previously noted, forward directivity effects from the 4 September 2010 Darfield earthquake are most evident in ground motions observed in the near-source region to the east of the causative faults. Figure 16 illustrates the observed velocity time histories at Templeton (TPLC), Rolleston (ROLC), and Lincoln (LINC), in which forward directivity effects are clearly evident. At both ROLC and LINC, peak ground velocities (PGV's) exceed 100 cm/s in the fault normal direction, as compared to approximately 60 cm/s in the fault parallel direction; while at Templeton (TPLC), PGV's are approximately 80 and 30 cm/s in the fault normal and parallel orientations, respectively.

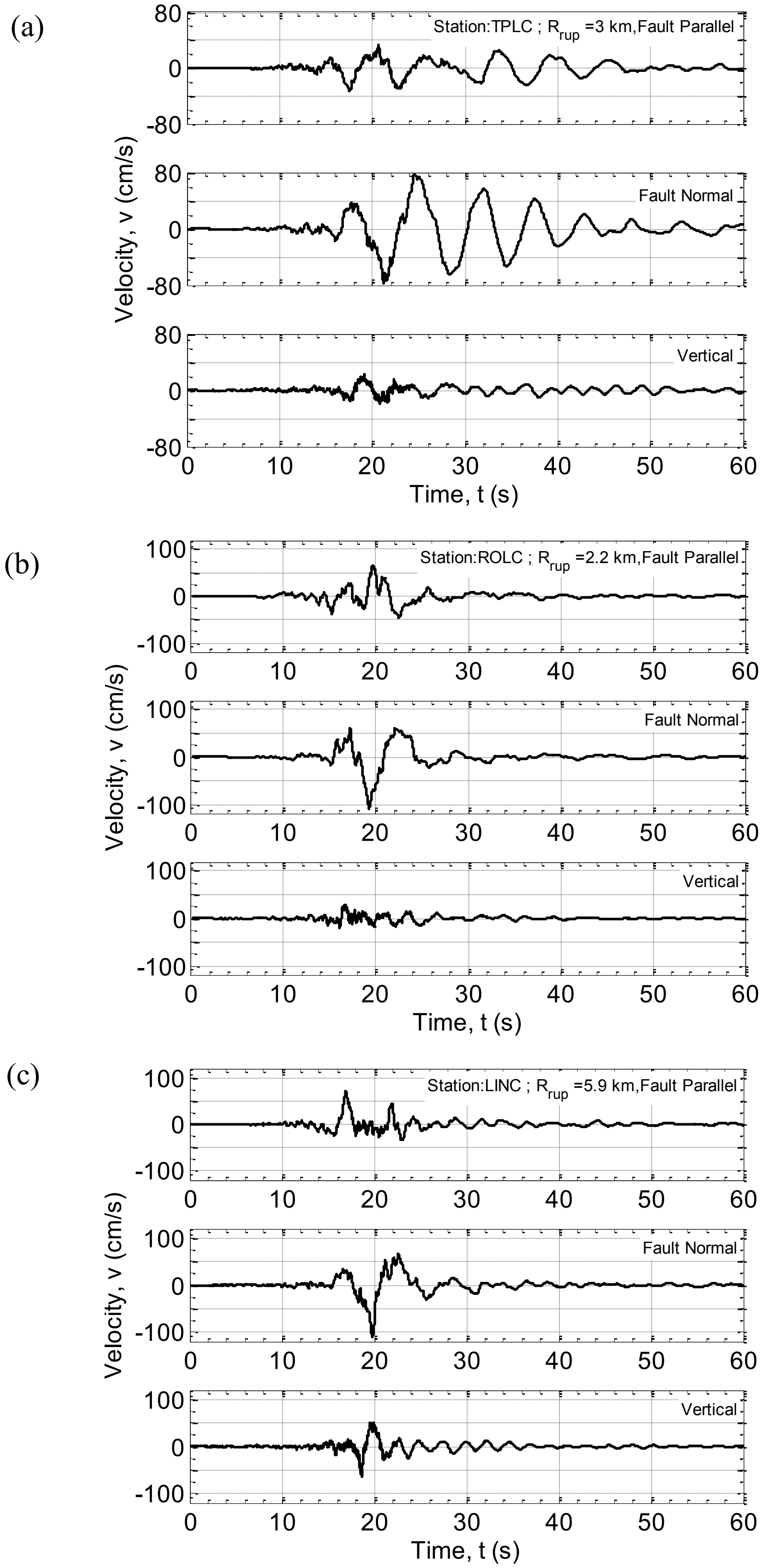

Figure 16: Evidence of strong forward directivity effects at locations to the east of the Greendale fault: (a) Rolleston (ROLC); (b) Lincoln (LINC); and (c) Riccarton (RHSC) resulting from the 4 September 2010 earthquake.

In addition to the clear evidence of forward directivity in ground motions located in close proximity to the eastern extent of the Greendale fault, such effects were also clearly discernable throughout the majority of Christchurch city. Figure 17 illustrates the fault normal component velocity time histories observed at the four strong motion stations located in the Christchurch central business district (CBD). It can be seen that the characteristics of the forward directivity velocity pulse are remarkably similar at all stations with PGV's ranging between 62 cm/s (CBGS) and 74 cm/s (CCCC). In contrast, the time history subsequent to the arrival of the velocity pulse varies significantly between the various sites illustrating the importance of both wave scattering and also shallow and deep geologic structure on site-specific site response (the sites are known to be located in areas with different near-surface geotechnical characteristics, despite all being nominally site class D [39, 40]).

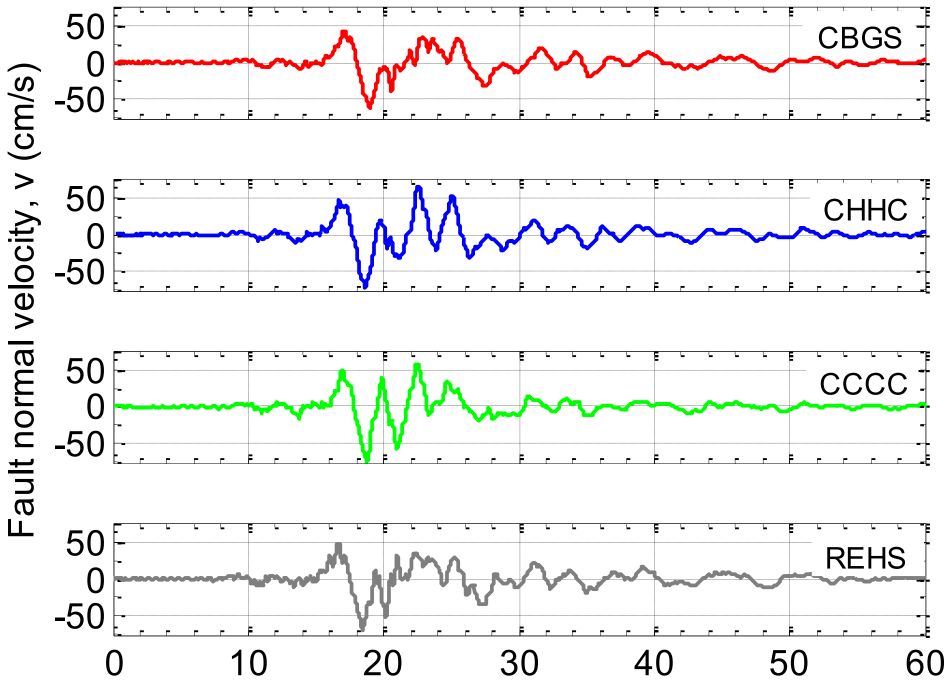

Figure 17: Forward directivity effects in the fault normal component observed in the Christchurch central business district (CBD) resulting from the 4 September 2010 earthquake.

Figure 18a illustrates the pseudo-acceleration response spectra (SA) of the fault normal time histories given in Figure 17. The effect of the large velocity pulses can be seen in the increased SA amplitudes at long periods. Very large spectral ordinates at $T \approx 2.5s$ can be seen in the response spectra of the CCCC and CHHC records, which had the largest pulse PGV's in Figure 17. In contrast, such a large increase in SA amplitudes is not observed at REHS and CBGS. At REHS, the SA peak resulting from the velocity pulse occurs at $T \approx 1.5s$, while there is no clear peak for CBGS. Despite this lack of a narrow SA peak at CBGS it should be noted that the fault normal SA amplitudes are still on the order of 3 times those in the fault parallel component over $T = 2 - 3$s, indicating that in this case the amplification from the forward directivity effect simply occurs over a wider range of vibration periods than the narrow range in the case of CCCC and CHHC (which have fault normal SA amplitudes approximately 5 times that in the fault parallel component for $T = 2.5$s as shown in Figure 18b). The comparison in Figure 18a clearly illustrates the variability in the period range and amplification factor due to forward directivity effects at four stations, all of which have essentially the same source-to-site geometry from the causative fault, and hence the complexity in modelling such phenomena using empirical approaches [e.g. 18].

Figure 18b illustrates the difference between the fault normal and fault parallel SA amplitudes at CHHC and CCCC. As noted previously, there is a ratio of SA amplitudes of the fault normal and parallel components of approximately 5 at the spectral peak of $T = 2.5$s. Examination of the fault parallel SA amplitudes illustrates additional SA peaks at $T \approx 3$ seconds, particularly evident for CHHC, and inferred as a result of basin-generated surface waves. Hence, in the fault normal direction, the large SA amplitudes at long periods are the result of both forward directivity (predominant effect) and also basin-induced surface waves (secondary effect), particularly at periods significantly larger than the directivity pulse period (i.e. $T \gg 3s$). For comparison, Figure 18b also illustrates the conventional 475-year return period response spectra prescribed for site class D soil conditions in Christchurch in the New Zealand loadings standard [12], as well as the maximum prescribed increase in the design spectra due to near-fault forward directivity effects. It can be seen that the maximum permissible increase in the design code response spectra (based on assuming a distance of less than 2km from the fault to the site), significantly under predicts the amplification of fault normal SA amplitudes relative to those in the fault parallel orientation, despite the fact that the Christchurch CBD is approximately 15km from the inferred eastern extent of the Greendale fault. Furthermore, it can be seen that the NZS1170.5 near fault factor produces an amplification over a broad period range, relative to the more narrow range over which significant amplifications are observed in Figure 18. Finally, it is noted that the near-fault amplitude specified by NZS1170.5:2004, as shown in Figure 18 is based on Somerville et al. [41] geometric mean forward-directivity amplification. This geometric mean amplification model should be used only for application to the geometric mean response spectral predictions. For NZS1170.5:2004, where the 'larger component' definition is used, the use of the Somerville et al. geometric mean forward directivity amplification is inappropriate. Somerville et al. also provide a model for the ratio of the fault normal to geometric mean components, and it is the product of these two models which should be used for consistency with NZS1170.5:2004. While changes to the near-fault factor in NZS1170.5:2004 are certainly warranted, it is noted that the Somerville et al. 'broadband' model is not outdated by several newer 'narrowband' models [e.g. 18].

It is pertinent to note that the effects of forward directivity were evident throughout Christchurch city in the 4 September 2010 earthquake with, for example, a velocity pulse in the fault normal direction with a PGV of approximately 50 cm/s clearly evident at New Brighton (NNBS) station. The NNBS station has a source-to-site distance of R_{rup} = 23.1km from the Greendale fault, clearly illustrating that the 'near-fault' region extends significantly beyond the 10-15km that is often conventionally considered as a bounding distance in many studies, and the value of 20km which is used as the bounding distance in NZS1170.5:2004, beyond which near-fault factors are not applied. The forward directivity effects discussed above with respect to the 4 September 2010 earthquake are not explicitly considered in the Bradley [7] and McVerry et al. [22] GMPEs. This is the principal reason for the under-prediction of the SA(3s) amplitudes from the 4 September 2011 earthquake that are annotated in Figure 13. As noted above, such effects should be explicitly considered in seismic hazard analyses, including those that underpin seismic design standards in future.

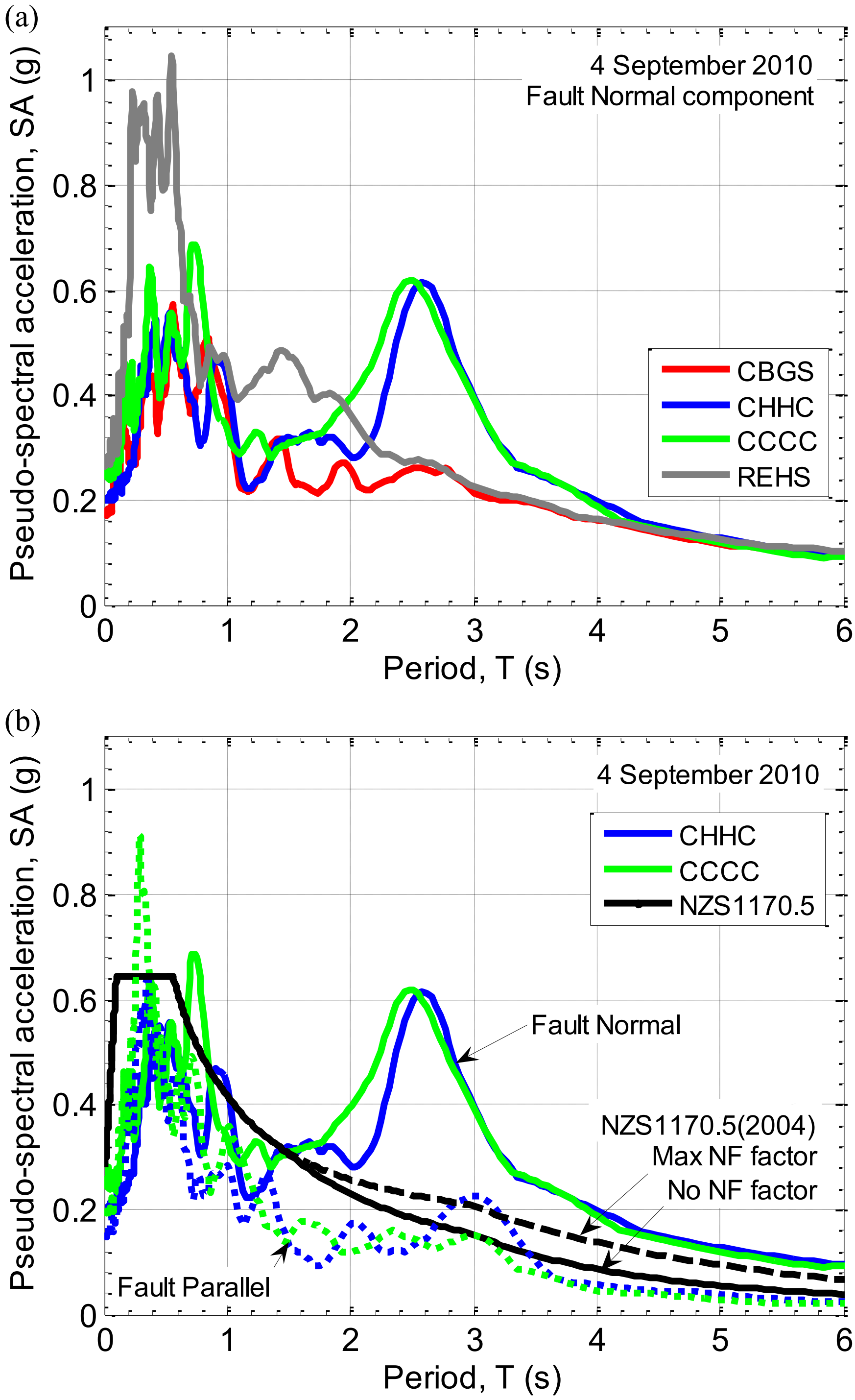

Figure 18: Illustration of the effects of forward directivity effects on: (a) the fault normal component response spectra at four CBD stations in the 2 September 2010 earthquake; and (b) the difference between response spectra in the fault normal and fault parallel components, relative to that prescribed in seismic design guidelines.

As previously noted, because of the mis-alignment of the directions of predominant fault slip, and the direction of rupture propagation in the 22 February 2011 Christchurch earthquake, it is expected that rupture directivity effects will only be important over a small area of the earth's surface, relative to other possible rupture scenarios [38]. This is in contrast to forward directivity effects in the 4 September 2010 Darfield earthquake discussed above, in which strike-slip rupture occurred bilaterally on the Greendale fault and forward directivity effects were significant for all locations in Christchurch city [35]. Figure 19a illustrates the three component velocity time history at Pages road (PRPC), where forward directivity effects can be seen in the fault-normal component manifested as the large ground velocities of low frequency, which cause a PGV of approximately 100 cm/s in the fault-normal component, while the fault-parallel component PGV is approximately 40 cm/s. This is further evident in the polar plot of the velocity trajectory at PRPC in Figure 19c (similar results are seen for the Darfield earthquake ground motions previously discussed). Figure 19b illustrates the three component velocity time history at Christchurch hospital (CHHC) where a velocity pulse in the fault normal component is not clearly evident (although there is some evidence in the fault-parallel component indicating complex rupture), and many of the large velocity amplitudes are the result of surface waves (elaborated upon subsequently). Again the lack of a strong forward directivity effect is evident in the velocity trajectory shown in Figure 19d, in which no clear polarity of large amplitude velocity is observed in the fault normal direction, and in fact the peak velocity is observed in the fault parallel component. The results of Figure 19b and Figure 19d do not imply that forward directivity is not important in the 22 February 2011 earthquake, only that its significance is less than in the case of the 4 September 2010 earthquake.

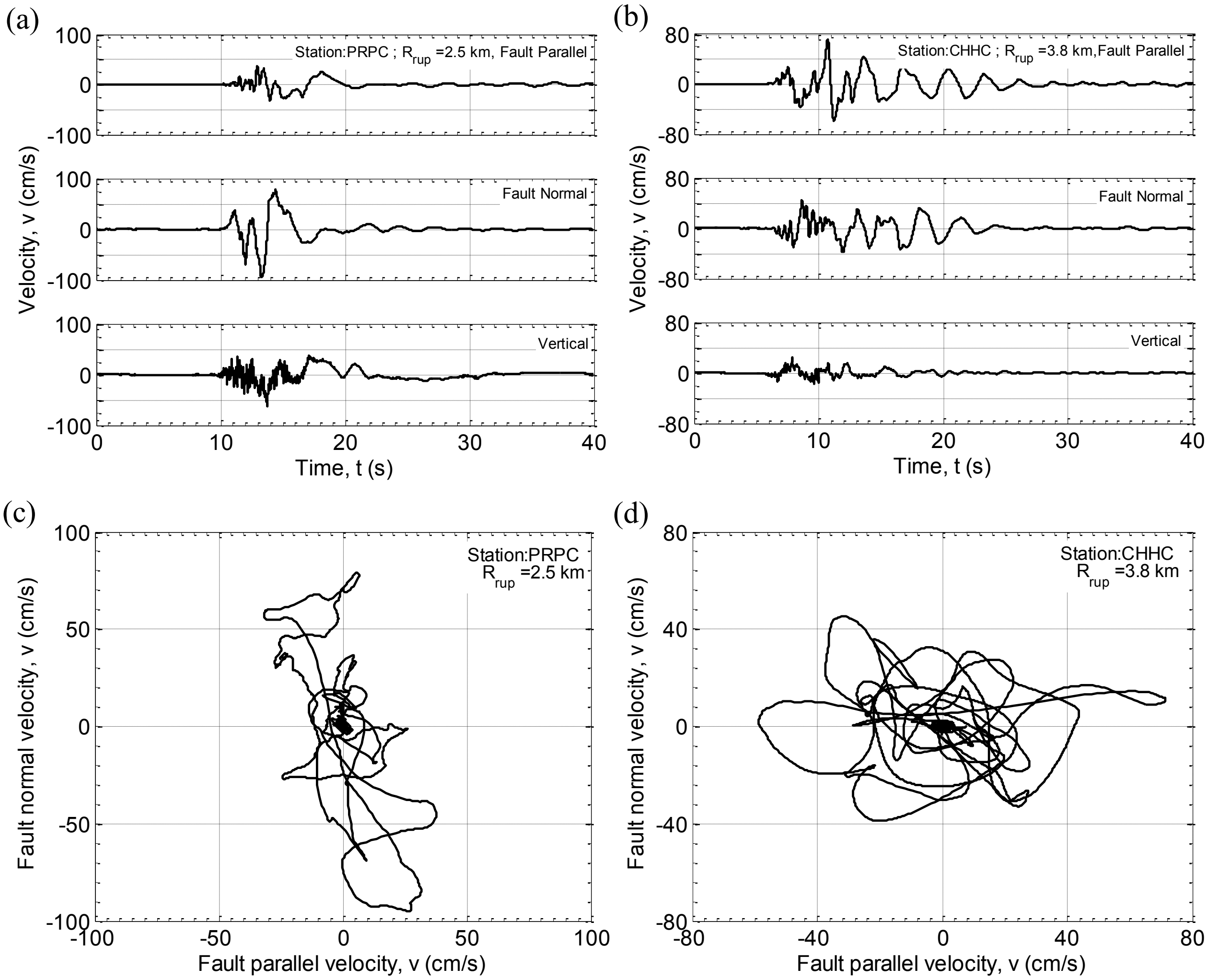

Figure 19: Velocity time histories and corresponding horizontal trajectory of fault normal and fault parallel velocity trajectory at Pages Road (PRPC) and Christchurch Hospital CHHC) from the 22 February 2011 Christchurch earthquake.

The significance of directivity effects on observed ground motions at a site are a function of the manner in which the causative fault ruptures (i.e. hypocentre location, slip vector and source-to-site azimuth). Because of the inability to exactly know such fault rupture characteristics, Archuleta

[32] notes that directivity can simply be considered within the variability of GMPEs, and not have specific functions within the GMPE which attempt to model it explicitly. The author disagrees with such an approach. Firstly, it must be recalled that GMPEs are empirical and based on an empirical database of historically recorded ground motions. Hence, if directivity effects are not well represented in the ground motion database, then they will not be well represented within the developed GMPE (neither in the median or standard deviation of the model). Because directivity effects are most pronounced at locations which are close to large magnitude earthquakes, and such recordings are rare, then typically directivity effects are not well represented by empirical data alone, and are more appropriately considered using semi-empirical models which combine empirical data with simple functions based on a fundamental understanding of the physics of directivity (e.g. Somerville et al. [41] or Shahi and Baker [18]).

An appropriate and pragmatic approach for consideration of directivity is to model directivity explicitly within ground motion modelling (e.g. 'add-on factors' which can be applied to conventional GMPEs which do not account for directivity are given by Shahi and Baker [18]), and to account for the uncertainty within the source parameters with probabilistic distributions. For example, as most engineering-based models for directivity require only the hypocentre location on the fault, in addition to information that is already required, then one can simply assign a probability distribution for the hypocentre location on the fault (typically a uniform distribution). Modelling directivity with the use of a uniform distribution for hypocentre location still gives different results than neglecting directivity since the increase in ground motion intensity due to forward directivity is more pronounced than the decrease in ground motion intensity due to backward directivity [e.g. 18].

4.3.2. Sedimentary Basin-generated Surface Wave Effects

Christchurch is located on a sedimentary fan deposit with the volcanic rock of Banks peninsula located to the south east. While specific mechanical and geometrical details of the predominant sedimentary basin layers are not well known, previous investigation has revealed the depth of gravel layers is in excess of 500m, with basement rock inferred to be at depths in excess of 2.0km at various locations [35, 42]. Significant long period ground motion was observed at numerous sites in the 4 September 2010 and 22 February 2011 earthquakes resulting from surface wave generation, in addition to the large amplitude long period ground motion resulting from forward directivity associated with source rupture effects.

In the case of the 4 September 2010 Darfield earthquake, large amplitude surface waves are the result of the shallow incidence angle at which seismic waves enter the basin-basement rock interface particularly associated with large fault slip at shallow depths. These shallow incidence angles consequently lead to post-critical angles upon reflection causing total internal reflection and essentially 'trapping' seismic waves within the basin layers, which consequently leads to a higher amplitude and longer duration of long period ground motion. Figure 16a, for example, illustrated that the velocity pulse associated with forward directivity at TPLC was subsequently followed by several cycles of basin-generated surface waves (with periods of approximately $T = 6$s), which are strongest in the fault normal component, consistent with the strongest SH waves in this component, but also evident in the fault parallel and vertical component velocity time histories. In contrast, the effects of surface waves are relatively small at ROLC and LINC in Figure 16b and Figure 16c, respectively. To aid in the examination of surface wave contribution in the observed time histories, Figure 20 illustrates approximate contours of basement rock depth in the Canterbury region [42]. It can be seen that basement rock outcrops to the west in the Southern Alps and within Banks Peninsula to the southeast of Christchurch city. While some caution is warranted in over-interpretation of the depth contours, given the data upon which they are based, the gross features of Figure 20 illustrate that the greatest basin depths occur near the TPLC station when taking a crosssection in the NW-SE direction through this location (on the order of 1.0km), and that basin depth further increase in the NE direction toward Kaiapoi (KPOC), and the Pegasus basin, which has basement rock at a depth in excess of 2.0km. Hence from Figure 20 it can be inferred that the notably lower amplitude of surface waves at LINC (in contrast to TPLC, for example) can be at least partially attributed to a shallower basement depth at this location, which is located to the west of the outcropping basement rock in Banks Peninsula. As a result of the directivity of rupture propagation and the basin geometry, Figure 20 also illustrates the occurrence of a waveguide effect which acts to efficiently propagate (i.e. with low effective geometric attenuation) long period surface waves through the western, central and northern regions of Christchurch. Figure 21 illustrates the velocity time histories observed at Styx Mill (SMTC), located in the north of Christchurch, and Kaiapoi (KPOC), located further north in the Waimakariri district. Despite their source-to-site distances of R_{rup} = 18km and 28km, respectively, it can be seen that the long period ground motion at SMTC and KPOC is significant with PGV's exceeding 40 cm/s when both scattered S- and surface-wave arrivals occur, and in excess of 30 cm/s later in the time histories when only surface waves are predominant. For Kaiapoi, in particular, it can also be seen that the vibration period of the surface waves is approximately 8 seconds, in contrast with approximately 6 seconds at SMTC and TPLC, consistent with the greater basin depths at this location. As expected from theory, it can also be observed when comparing the velocity time histories at TPLC, SMTC and KPOC that surface waves velocity amplitudes increase relative to those occurring during the majority of S-wave arrivals with increasing source-to-site distance.

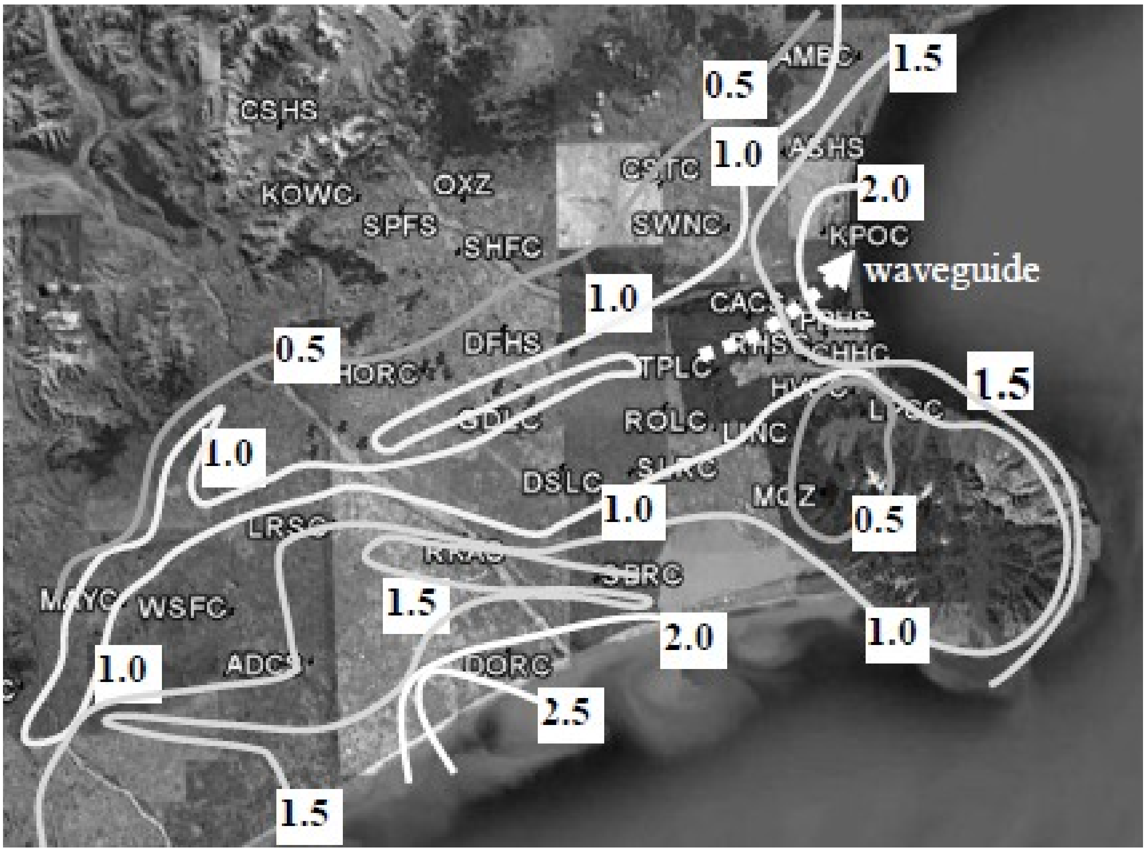

Figure 20: Depth to basement rock (in km) in the Canterbury region [42], and relationship to observed waveguide effects [35].

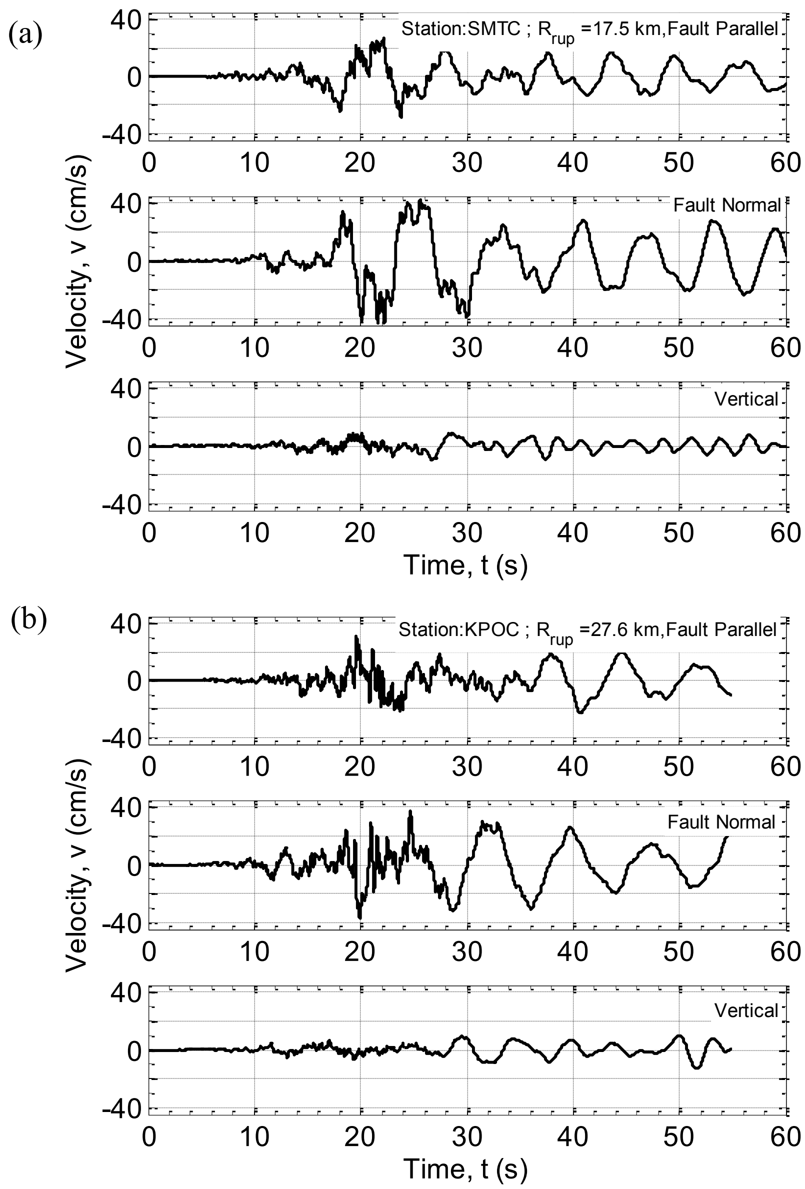

Figure 21: Illustration of significant basin generated surface waves from the 4 September 2010 earthquake: (a) Styx Mill (SMTC); and (b) Kaiapoi (KPOC).

Basin-generated surface waves were also evident at various locations from the 22 February 2011 earthquake, as depicted at four locations in Figure 22. At close source-to-site distances clearly discerning surface wave contribution is not trivial due to the overlap in time of the first surface wave arrivals and scattered S-waves. Both Papanui (PPHS) and Styx Mill (SMTC) however illustrate several long period oscillations subsequent to the majority of S-wave arrivals. The significance of basin-induced surface waves becomes more visible and predominant as the distance from the causative fault increases, both as a result of the different wave propagation velocities of the body and surface waves (so they arrive at different times and are easier to visually bracket), and also because of the fact that body waves geometrically attenuate at a higher rate (R^{-1}) than surface waves ($R^{-1/2}$) with distance. As a result, it can be seen in Figure 22 that, at both Templeton (TPLC) to the west of Christchurch, and Kaiapoi to the north, the duration and amplitude of the surface waves relative to body waves significantly increases. At KPOC in particular, it can be seen that despite being 20km from the causative fault, high frequency ground motion occurs followed by significant surface wave amplitudes with PGV's up to 20 cm/s.

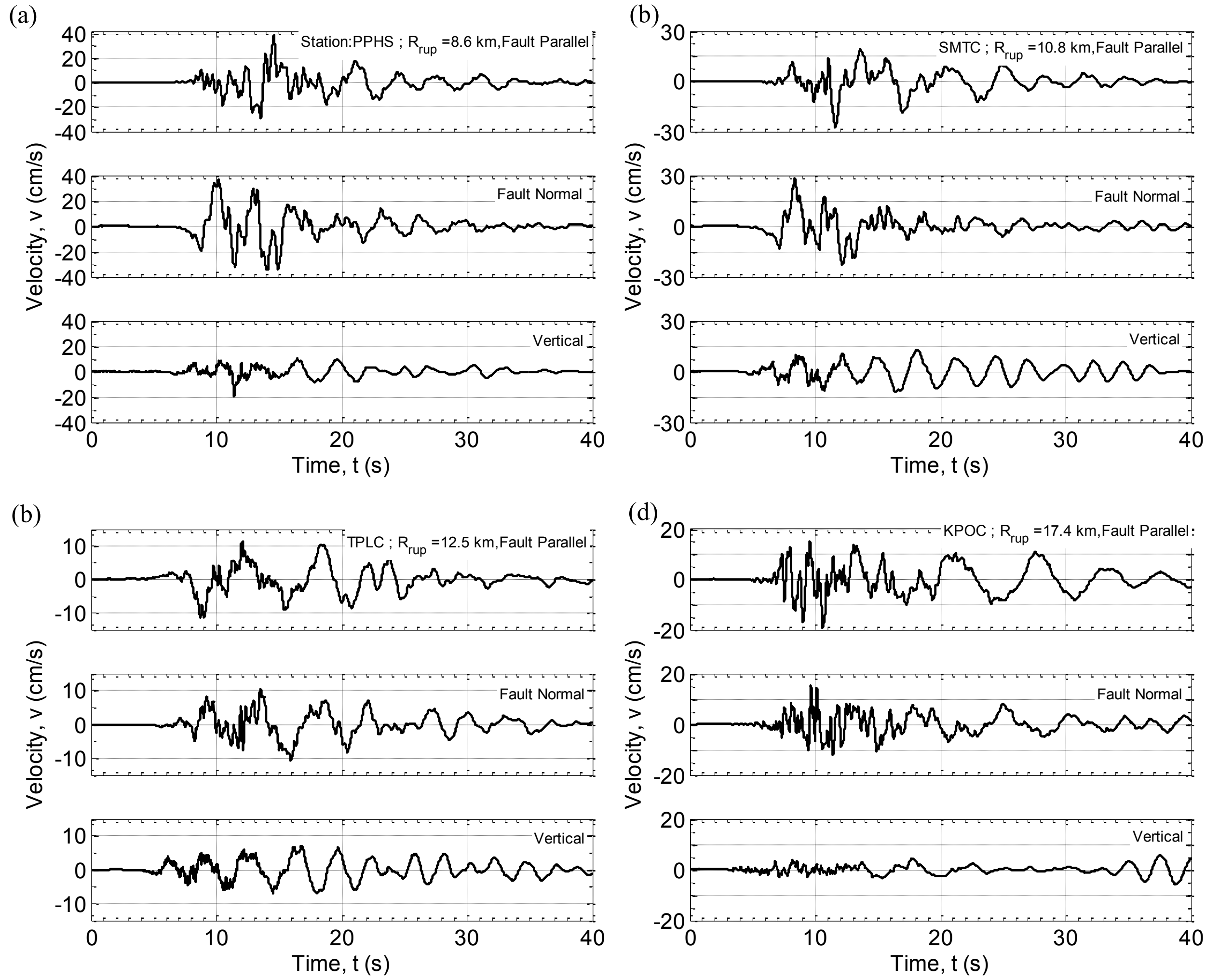

Figure 22: Velocity time histories illustrating the significance of basin-generated surface waves in the 22 February 2011 earthquake: (a) Papanui (PPHS); (b) Styx Mill (SMTC); (c) Templeton (TPLC); and (d) Kaiapoi (KPOC).

With respect to ground motion modelling, it is emphasised that GMPEs that do not consider parameters which are known to affect the significance of basin-induced surface waves (such as basin depth, or fundamental vibration period of the basin) will only be able to accurately model these effects if they are well accounted for in the database of ground motions upon which the empirical GMPE is developed. It should be noted that as basin waves become more signficant as the magnitude of the causative earthquake increases (all other things equal), and large magnitude earthquakes occur infrequently, then it can be expected that large amplitude ground motions with signficant basin-induced surfaces will not be well represented in empirical databases. Therefore, as in the case of forward directivity, semi-empirical models for consideration of basin-induced surface waves are recommended as opposed to simply suggesting that such effects are implicitly accounted for within the empirical database used in GMPE development.

4.3.3. Nonlinear Response of Near-surface Soil Deposits

Another significant contribution to long-period ground motion amplitudes is the additional amplification from nonlinear soil behaviour. While empirical ground motion models do consider soil classification, the manner in which they do is extremely rudimentary (see section 4.1.1). In addition to the use of simplistic alphabet-based site classifications, because of the fact that very strong ground motions are observed far less frequently than moderate and weak ground motions, empirical GMPEs often contain few (if any) ground motions which have resulted from signficant nonlinear response in surficial soil layers. Therefore the accuracy and precision of GMPEs for predicting ground motion amplitudes at sites where signficant nonlinear response of surficial soil response is anticipated is notably poorer than sites where such response is not expected.

A self-evident illustration of the significance of nonlinear soil response is possible from a comparison of two ground motions recorded at Lyttelton Port during the 22 February 2011 earthquake [36, 37]. One of the obtained from motions is located on 'engineering' bedrock (LPCC), while the other is located on a relatively thin (~30m) colluvium layer [36]. Figure 23 illustrates the acceleration time histories in three components at each of these two locations. It can evidently be seen that the horizontal components of ground motion at the soil site have significantly lower amplitude, but are of longer period, than those at the rock site. In contrast, the vertical accelerations at the two locations are similar. Figure 24 illustrates the pseudo-acceleration response spectra of the geometric mean horizontal and vertical ground motion components at the two sites. It can be seen that the observed horizontal ground motion at the LPOC site has significantly lower short period ground motion amplitude, but notably larger response spectral amplitudes at longer periods. The vertical response spectra can be seen to be very similar, as was evident from comparison of their time histories.

The reduction of short period ground motion, and amplification of long period ground motion has important implications for structures. For short period structures (e.g. residential housing, and 1-2 storey commercial structures) the effect of nonlinear soil response is a reduction in the spectral accelerations. For moderate-to-long period structures (particularly structures in the range 5-15 storeys), the effect of nonlinear soil response is a significant increase in the spectral acceleration. It also should be noted that in addition to nonlinear soil response leading to modification of the surface ground motion, it also typically results in unacceptably large ground deformations, which can place extreme demands on the foundations of structures. Therefore, the reduction in short period ground motion as a result of nonlinear soil response should not be considered as beneficial for structural design. Further discussion on nonlinear soil response (including liquefaction) and its importance for structures and foundations may be found in Cubrinovski and McCahon [43], among others.

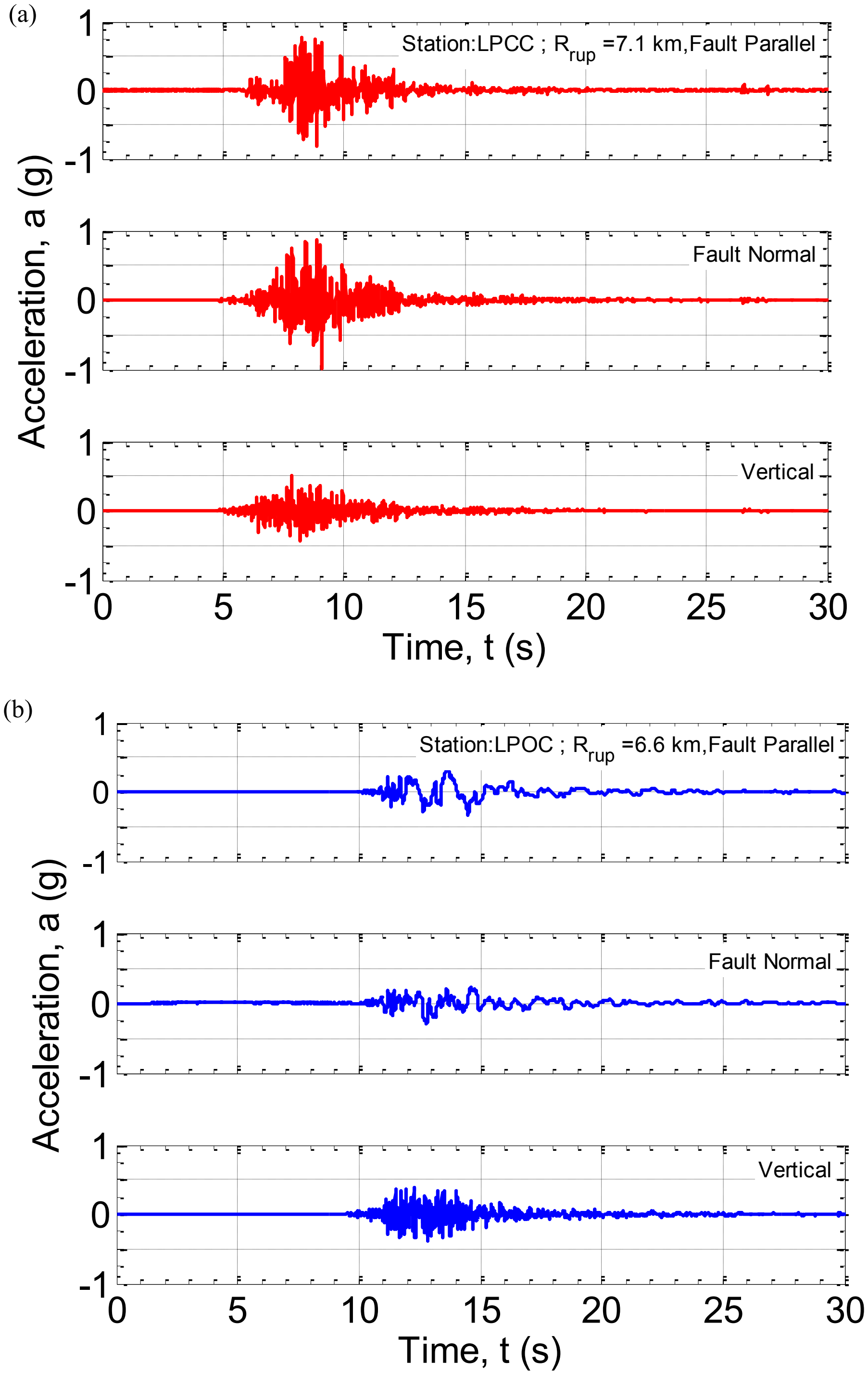

Figure 23: Comparison of the acceleration time histories recorded at Lyttelton Port during the 22 February 2011 earthquake illustrating the importance of surficial soil response: (a) LPCC (rock); and (b) LPOC (soil).

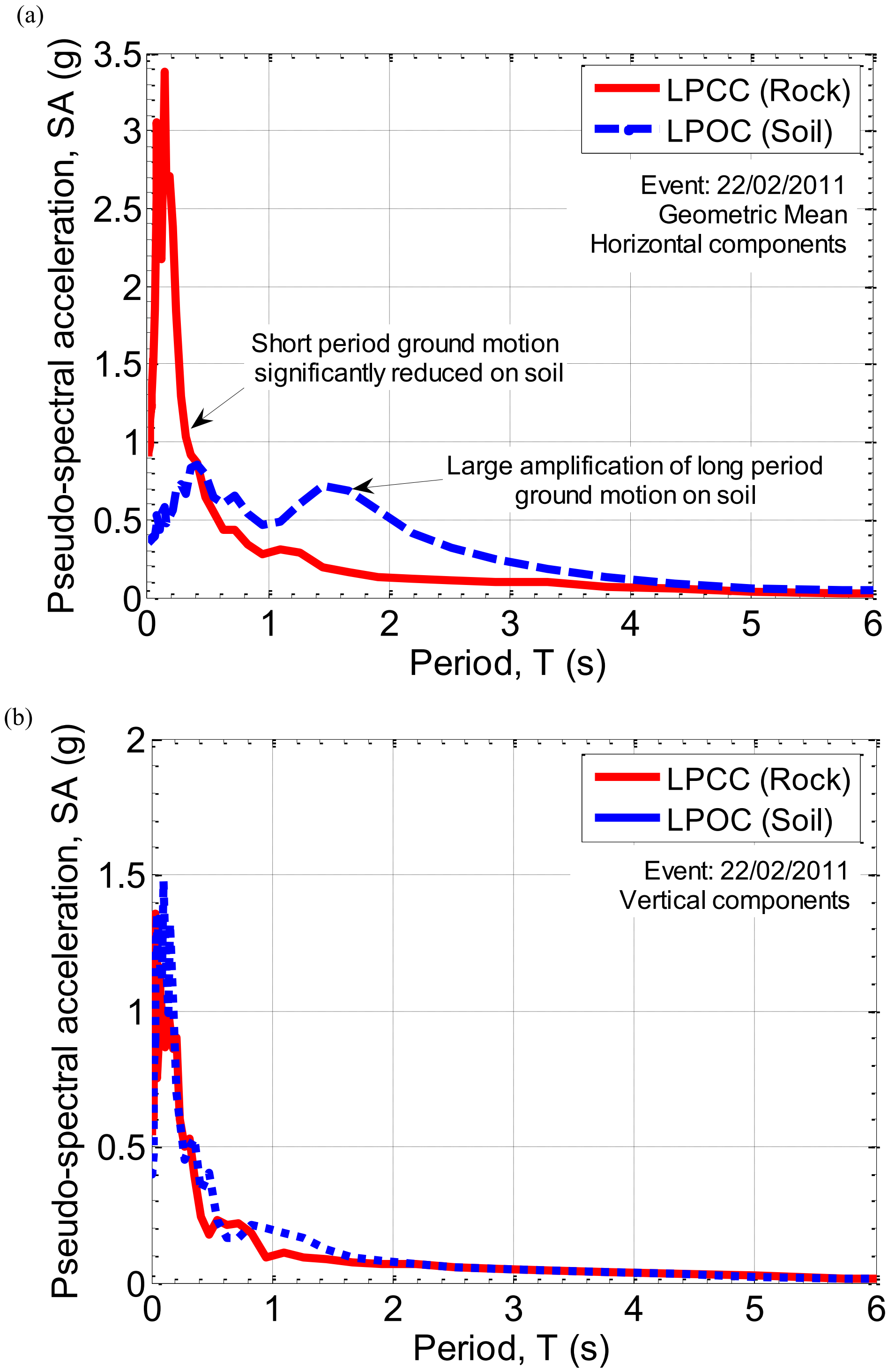

Figure 24: Comparison of the ground motion response spectra at Lyttelton Port during the 22 February 2011 earthquake illustrating the importance of surficial soil response: (a) geometric mean horizontal component; and (b) vertical component.

In addition to the above comparison at Lyttelton Port, large long period ground motion response spectral ordinates were also observed in Christchuch during the 22 February 2011 earthquake, in particular, in the central business district (CBD). As previously noted, such high amplitude long period ground motion is also the result of forward directivity, and trapping of basin-induced surface waves, in addition to the effect of nonlinear soil response. It is prudent to expect that future earthquakes in the wider Canterbury region, which have the potential to produce strong ground motion in Christchurch, will contain strong long-period ground motion from nonlinear soil response and signficant basin-induced surface waves, since these are properties of the Christchurch geology (although the incident direction of seismic waves will affect basin-induced surface waves). Near-source forward-directivity effects will obviously be dependent on the relative location of Christchurch to causal ruptures, and are not likely to be significant for earthquakes in the Canterbury foothills and Southern Alps (e.g. Porters Pass, Hope, and Alpine faults).

4.3.4. Vertical Ground Motion Response Spectral Intensities

Large ground motions were observed in the vertical component at various locations in both the 4 September 2010 and 22 February 2011 earthquakes. Such large vertical accelerations can be understood physically, because the majority of strong motion stations are located on soil sites, and for soil sites in sedimentary basins large vertical accelerations at near-source locations can result from the conversion of inclined SV-waves to P-waves at the sedimentary basin interface which are subsequently amplified and refracted towards vertical incidence due to the basin P-wave gradient [44]. That is, large vertical accelerations observed at near-source locations are expected, and are not an indication on their own of any peculiarities associated with the earthquake source.

Figure 25 illustrates the ratio of peak vertical acceleration and peak horizontal acceleration observed at the near-source strong motion sites in the Christchurch earthquake. For comparison, the empirical model of Bozorgnia and Campbell [45] is also shown. It can be seen that peak vertical-to-horizontal ground acceleration ratios of up to 4.8 were observed. The peak vertical-to-horizontal ground acceleration ratios show a rapid decay with source-to-site distance and it can be seen that the observed ratios compare favourably with the Bozorgnia and Campbell empirical model for source-to-site distances beyond 5km, but significantly under-predict the ratios at closer distances. In Figure 25, data are also differentiated by whether liquefaction was observed at the location of the ground motion instrument [36]. It can be seen that almost all strong motion records at distances less than 5km show liquefaction evidence (the exception being HVSC). At the aforementioned sites (with source-to-site distances are less than 5km), the large peak vertical-to-horizontal ground acceleration ratios observed are interpreted to be the result of significant non-linear soil behaviour (including liquefaction) which generally results in more of a reduction in peak horizontal accelerations than peak vertical accelerations (e.g. as seen in Figure 24).

To explore the results in Figure 25 in more detail, and provide addition insight, Figure 26a illustrates the geometric mean horizontal pseudo-acceleration response spectra at PRPC, CHHC and RHSC, and Figure 26b the corresponding vertical-to-horizontal ratios. As has been commonly observed in numerous other studies, it can be seen that the vertical-to-horizontal (V-to-H) spectral ratio is largest at high frequencies with values that can be significantly greater than 1.0, and tends to reduce rapidly for vibration periods greater than $T = 0.1$s, and as a function of source to site distance (i.e. $R_{rup} = 2.5$km, 3.8km, and 6.5km for PRPC, CHHC, and RHSC, respectively [36]). Figure 26c-Figure 26f illustrate the V-to-H spectral ratios for four different vibration periods, $T = 0.0$, 0.1, 0.2, and 0.3s as a function of source-to-site distance for both the 22 February 2011 Christchurch and 4 September 2010 Darfield earthquakes. Also shown for comparison is the empirical model of Bozorgnia and Campbell [45], and the prescribed ratio of 0.7 for the development of vertical design spectra in NZS1170.5 [12]. Firstly, it can be clearly seen that V-to-H ratios above 1.0 are frequently observed for distances up to $R_{rup} = 40$km in both these events (as well as other historical earthquakes worldwide [45]), and hence the code prescription of 0.7 is significantly un-conservative. Secondly, it can be seen that while there is significant scatter in the observed ratios, the Bozorgnia and Campbell empirical model is able to capture the overall trends in the observations, except for $R_{rup} < 10$km for which it underestimates the observed ratios. Comparison of the observations from the Darfield and Christchurch earthquakes also illustrates that the ratios, on average, are principally a function of source-to-site distance and there is no evidence for a systematic differences between the two events due to their different magnitude and style of faulting. This lack of average dependence the seismic source features is consistent with that of Bozorgnia and Campbell [45]. Comparison of the ratios observed at the same station in the two different events (annotated in the figures for PRPC and HPSC) illustrates that there is some systematic site effect, for example, HPSC is always above the average prediction, but this is not always the case for PRPC with the ratio for $T = 0.2$s well above the prediction in the Christchurch earthquake, but below the prediction in the Darfield earthquake. Given that vertical ground motion is only significant at very high frequencies, then it is expected to be strongly correlated with near-surface P-wave velocity structure, and some of the fluctuations observed in Figure 26 are likely the result of variability in the amplitude of the horizontal ground motion on the V-to-H ratio (due to nonlinearities for example).

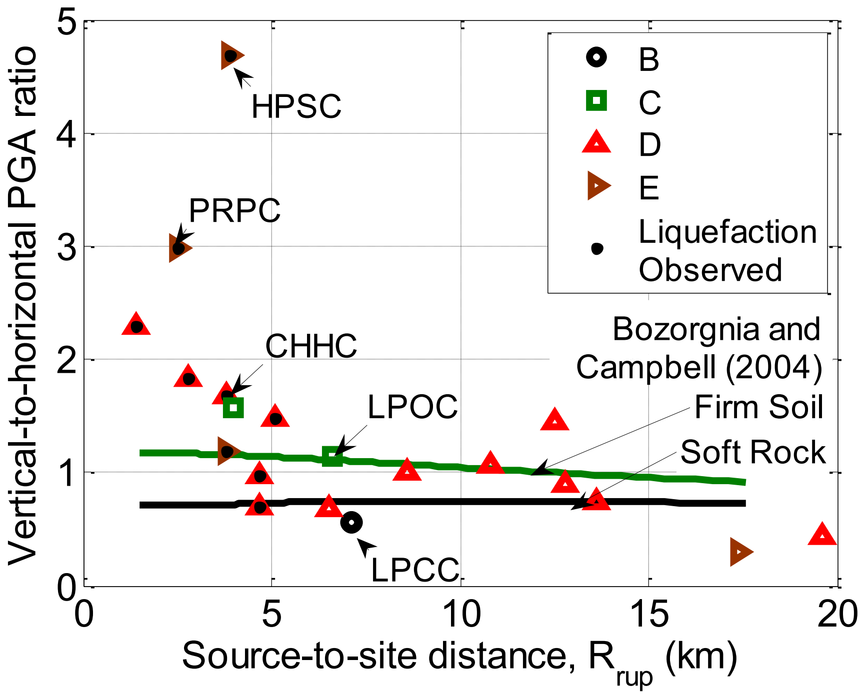

Figure 25: Observed vertical-to-horizontal peak ground acceleration ratios as a function of source-to-site distance in comparison with the empirical equation of Bozorgnia and Campbell [45]. Data are differentiated by site class as well as evidence of liquefaction.

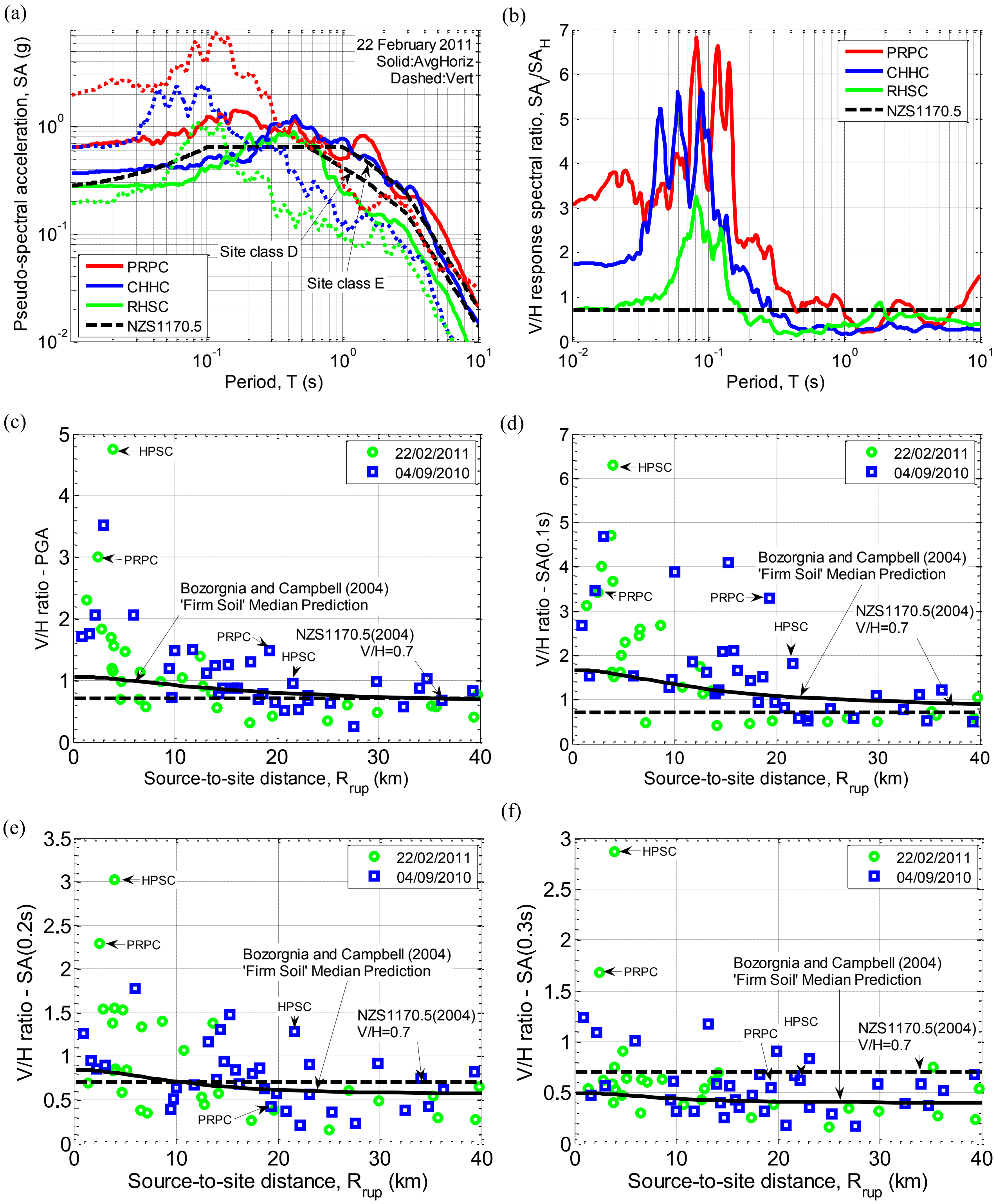

Figure 26: Vertical ground motion response spectral amplitudes observed: (a)-(b) Example geometric mean horizontal and vertical response spectra and their vertical-to-horizontal ratio; (c)-(e) vertical-to-horizontal response spectral ratios for T = 0.0-0.3s as a function of distance observed in the 4 September 2010 Darfield and 22 February 2011 Christchurch earthquakes and comparison with the empirical prediction of Bozorgnia and Campbell [45].

The above discussions serve to illustrate that the large number of observed strong vertical ground motions in the 22 February 2011 Christchurch earthquake is principally a result of a larger number of recordings at very small source-to-site distances relative to the Darfield earthquake (e.g. 15 records within 10km in the Christchurch earthquake as compared with 8 in the Darfield earthquake), rather than any specific source effect during rupture in the Christchurch earthquake. Finally, as horizontal ground motion amplitudes within Christchurch city in the Christchurch earthquake were larger than those from the Darfield earthquake, then nonlinear shear deformation of soils which results in a reduction of tangent shear modulus, and therefore the ability to propagate high frequency ground motion, was more significant in the 22 February event. Nonlinear shear deformation on the other hand does not have as significant an effect on the compressibility of soil, which is related to P-wave velocity, and hence vertical ground motion amplification. The significant effect of nonlinear site response on horizontal ground motion, yet minor effect on vertical ground motion, was clearly illustrated in Figure 23 and Figure 24.

Despite the above comments, and the recommendation that the seismic design provisions for vertical acceleration are un-conservative for short vibration periods in the near-source region, it should be recalled that vertical accelerations are not the principal cause of damage from earthquake-induced ground motion, Furthermore, vertical accelerations are not significant in the build up of pore-water pressures in soil deposits and consequent liquefaction, since vertical accelerations result in an increase in both total stress and pore water pressure, and hence do not significantly affect the effective stress which govern soil response. However, the fact that vertical accelerations are not the principal cause of damage to structures does not imply that they are not important. Several numerical modelling studies have shown that the consideration of vertical accelerations, in additional to horizontal accelerations, leads to incrementally higher demands in certain structural components [e.g. 46]. Furthermore, various components which are not part of the primary structural system (e.g. non-structural components, as well as stairwells etc.) may be sensitive to vertical accelerations, and therefore accurate design provisions are prudent.

4.3.5. Effects of Source-to-site Distance on Ground Motion Response Spectral Amplitudes

In addition to earthquake magnitude and surficial soil type, source to site distance can be regarded as a fundamental parameter which affects the characteristics (amplitude, frequency content, duration) of ground motions. Because seismic waves attenuate in amplitude via geometric spreading and anelastic attenuation then their amplitude generally decreases with distance. Near-source directivity effects also generally reduce with source-to-site distance. Lower ground motion amplitudes also reduce the significance of nonlinear response of surficial soils.

Figure 27 compares various observed horizontal response spectra in both the 22 February 2011 and 4 September 2010 earthquakes, which have varying source-to-site distances, with the Christchurch design spectra according to NZS1170.5:2004. In both earthquakes it can be seen that the ground motion in close proximity to the fault (i.e. $R_{rup} < 3km$) is very strong, well exceeding the 500year design response spectrum, and often the 2500year response spectrum also. As the source-to-site distance increases there is a general reduction in the ground motion amplitude due to geometric spreading and the consequent effects noted above. For example, at approximately 6km from the source of both earthquakes (i.e. RHSC in Figure 27a and LINC in Figure 27b) the ground motion is generally in the vicinity of the 500year design response spectra, although clearly this is a function of the vibration period considered. As the distance increases further to approximately 10-12km (i.e.

TPLC in Figure 27a and RHSC in Figure 27b) the ground motion response spectral amplitudes reduce further, and are below the 500year design response spectrum over a wide range of periods. It should be noted in particular, that for the larger 4 September 2010 earthquake (i.e. $M_w 7.1$ compared to $M_w 6.3$ for 22 February 2011), the reduction in ground motion amplitudes with distance is much less pronounced.

(a)

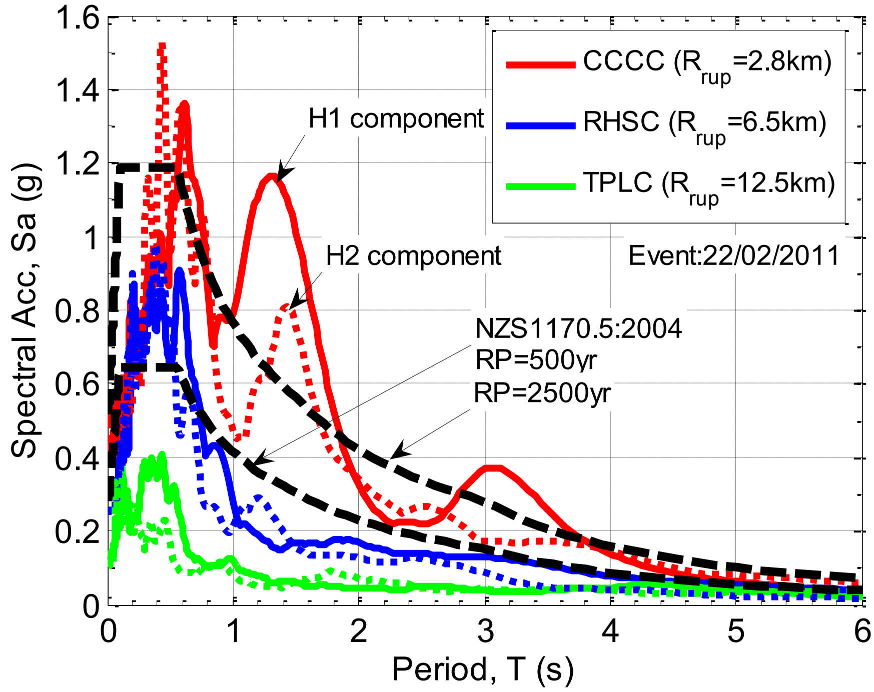

(b)

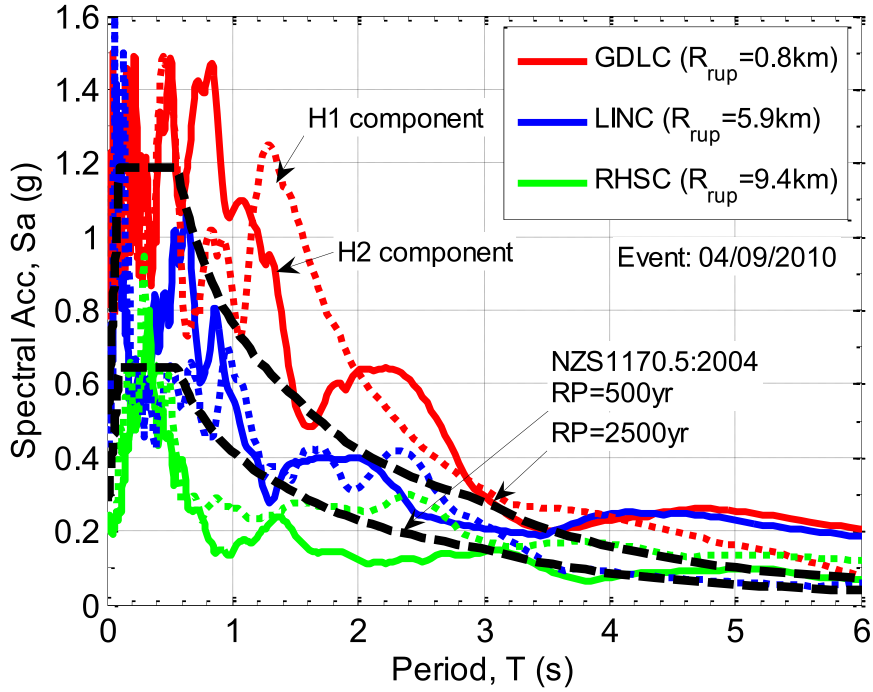

Figure 27: Comparison of ground motion response spectra illustrating the general trend of attenuation with source to site distance: (a) 22 February 2011; and (b) 4 September 2010 earthquakes. The NZS1170.5:2004 Site class D spectra are also shown for 500 and 2500 year return periods.

Note that because of the complexity of the source rupture, wave propagation and local site effects, the general trend of reducing ground motion intensity with distance is not systematic. For example, Figure 9-Figure 13 illustrated the attenuation of various response spectral amplitudes with distance where it could be seen that there is significant scatter in the general attenuation trend.

4.4. Recommended Modifications in Ground Motion Modelling

- Observed response spectral amplitudes in both the 22 February 2011 and 4 September 2010 earthquakes illustrates that the McVerry et al. [22] GMPE provides a poor predictive capability as compared to more recent GMPEs (such as the Bradley [7] model, and those available in literature [27]). As such, future seismic hazard analyses for New Zealand should avoid the use of the McVerry et al. model. Recent models, which are shown to be applicable to New Zealand, should be used (preferably several models in a 'logic tree' with weights reflecting perceived model suitability).
- The near-fault factor used in NZS1170.5:2004, to account for forward directivity, is inadequate for amplifying long period response spectral ordinates as compared with ground motion observations from the Canterbury earthquakes. Forward directivity effects can result from small-to-moderate magnitude earthquakes as well as large earthquakes [33]. Therefore, near-fault effects should be explicitly used in ground motion modelling (either via GMPEs that include near-fault effects, or using 'add-on factors') so that they are automatically included in the results of seismic hazard analyses, and therefore in design standards such as NZS1170.5:2004, rather than requiring the structural analyst to apply them as an additional modification of the prescribed design response spectrum.
- The McV06 ground motion model which underpins the results in NZS1170.5:2004 does not contain explicit account for 'basin effects', which can lead to a significant increase in the duration and long period content of strong ground motion. Basin effects will be most significant for large earthquakes, since they produce ground motions of long duration and strong long period ground motion intensity (relative to short period intensity); and also for earthquakes which are located adjacent to, rather than below, the sedimentary basin [47]. Hence, for example, signficant basin effects (more than that in the Canterbury earthquakes) would be expected for earthquake events in the southern Alps (e.g. the $\sim M_w 8.1$ Alpine fault, and the $\sim M_w 7.5$ Hope and Porters Pass faults), and also the Hikurangi Subduction Zone ($\sim M_w 8.8$). The predominance of basin effects on damage are well documented in past earthquakes, e.g., the 2003 Tokachi-Oki earthquake in Honshu, Japan [48].
- Nonlinear soil response can lead to significant amplifications of long period ground motion amplitudes which are not accurately represented in empirical GMPEs due to the variation in near surface soil deposits that arise, and their influence on this nonlinear response. The potential benefits of using site response analysis, in which the soil profile at the site is modelled directly rather than using broad soil classifications, should be emphasised in seismic design standards and relevant guidance prescribed.

- The simplistic provision that the vertical design spectrum is equal to 70% of the horizontal design spectrum is un-conservative in comparison with ground motions that result in the near-source region of the causal fault (even for small magnitude events, as the 22 February 2011 earthquake illustrates), and consequently requires revision.

5. Conclusions

This report has examined seismicity and ground motion aspects of the 22 February 2011 and 4 September 2010 earthquakes in the Canterbury earthquake sequence. In particular, the observed earthquakes and induced ground motions were examined with respect to the seismicity and ground motion models which are used to assess ground motion hazard in New Zealand, and in particular the New Zealand Seismic Loadings Standard, NZS1170.5:2004.

Section 2 provided an overview of seismic hazard analysis and design ground motions, which form the basis of NZS1170.5:2004. Particular emphasis was given to the discussion of probabilistic seismic hazard analysis (PSHA), which is the principal means by which the elastic design spectra in NZS1170.5:2004 are computed, and how the seismicity and ground motions that form components of PSHA can be validated based on earthquake and ground motion observations.

Section 3 examined the New Zealand seismicity model in the context of the Canterbury earthquake sequence. While the earthquakes in the Canterbury sequence occurred on unmapped faults, such 'off-fault' earthquakes are accounted for in 'background seismicity' within PSHA models. While the maximum background magnitude in the most recent New Zealand seismicity model allows for the possibility of earthquakes with magnitudes such as those of the Canterbury earthquake sequence, the New Zealand seismicity model currently considers such earthquakes as point sources, with a minimum depth of 10km. The use of point-sources in the seismicity model is inconsistent with the use of finite-fault based parameters in ground motion modelling which results in un-conservatively lower surface ground motions, particularly in the near-source region of signficant background earthquakes. The use of a minimum depth of 10km is also inconsistent with centroid depths in the Canterbury earthquakes, which are as low as 4km, and this also results in un-conservative estimates of ground motions at the surface.

Section 4 examined the strong ground motions observed in the Canterbury earthquakes in comparison with New Zealand-specific empirical ground motion models. It was seen that the commonly adopted ground motion model of McVerry et al. [22], provides a signficant over-estimation of response spectral amplitudes at short periods ($T \approx 0.2s$) and under-estimation at moderate-to-long periods for ground motions in the near-source region of the causal earthquake. The more recently developed New Zealand-specific model of Bradley [7], based on a significantly larger set of empirical ground motions, provides a significantly more consistent prediction when compared with the observed ground motions (particularly at short and moderate periods). Nonetheless, at long periods, the effects of forward directivity (particularly for the 4 September 2010 earthquake), basin-induced surface waves, and nonlinear response of surficial soils produce strong long period ground motion, which is either not explicitly modelled, or poorly constrained by empirical models. Observations, particularly from the 4 September 2010 earthquake, illustrate that that the NZS1170.5:2004 factor for forward-directivity effects is largely un-conservative and requires revision. Observations from both the 4 September 2010 and 22 February 2011 earthquakes illustrate that, in the near-source region and for short vibration periods, response spectral amplitudes of the vertical component of ground motion are notably larger than the 0.7 factor in NZS1170.5:2004, and therefore these prescriptions require revision. Nonlinear response of near-surface soils is also significant in the modification of surface ground motions. As nonlinear response is a function of the physical and mechanical properties of the surficial soils, clearly broad site classifications, as currently prescribed in NZS1170.5:2004, cannot capture nonlinear site effects with accuracy of precision.

6. References

[1] Youngs RR and Coppersmith KJ. Implications of fault slip rates and earthquake recurrence models to probabilistic seismic hazard estimates. *Bulletin of the Seismological Society of America* 1985; **75**(4): 939-964.

[2] Gutenberg B and Richter CF. Frequency of earthquakes in California. *Bulletin of the Seismological Society of America* 1944; 185-189.

[3] Field EH and Page MT. Estimating Earthquake-Rupture Rates on a Fault or Fault System. *Bulletin of the Seismological Society of America* 2011; **101**(1): 79-92.

[4] Parsons T and Geist EL. Is There a Basis for Preferring Characteristic Earthquakes over a Gutenberg–Richter Distribution in Probabilistic Earthquake Forecasting? *Bulletin of the Seismological Society of America* 2009; **99**(3): 2012-2019.

[5] Stirling MW, McVerry G, Gerstenberger M, Litchfield N, Van Dissen R, Berryman K, Barnes P, Beavan J, Bradley BA, Clark K, Jacobs K, Lamarche G, Langridge R, Nicol A, Nodder S, Pettinga J, Reyners M, Rhoades D, Smith W, Villamor P and Wallace L. National Seismic Hazard Model for New Zealand: 2010 Update. *Bulletin of the Seismological Society of America* 2011; **(submitted)**.

[6] Stirling MW, McVerry GH and Berryman KR. A new seismic hazard model for New Zealand. *Bulletin of the Seismological Society of America* 2002; **92**(5): 1878–1903.

[7] Bradley BA. *NZ-specific pseudo-spectral acceleration ground motion prediction equations based on foreign models*, Report No.2010-03, Department of Civil and Natural Resources Engineering, University of Canterbury: Christchurch, New Zealand, 2010. 324pp.

[8] Kramer SL. *Geotechnical earthquake engineering*. Prentice-Hall: Upper Saddle River, NJ. p. 653.

[9] Krinitzsky EL. How to obtain earthquake ground motions for engineering design. *Engineering Geology* 2002; **65**(1): 1-16.

[10] Cornell CA and Winterstein SR. Temporal and magnitude dependence in earthquake recurrence models. *Bulletin of the Seismological Society of America* 1988; **78**(4): 1522-1537.

[11] Bommer JJ. Deterministic vs. probabilistic seismic hazard assessment: An exaggerated and obstructive dichotomy. *Journal of Earthquake Engineering* 2002; **6**(1 supp 1): 43 - 73.

[12] NZS 1170.5. *Structural design actions, Part 5: Earthquake actions - New Zealand*. Standards New Zealand: Wellington, New Zealand, 2004, 82pp.

[13] Veletsos AS and Newmark NM. *Effect of inelastic behavior on the response of simple systems to earthquake motions*, in *Second World Conference on Earthquake Engineering*. Science Council of Japan: Japan, 1960, 895–912pp.

[14] Newmark NM and Hall WJ. *Earthquake spectra and design*. Earthquake Engineering Research Institute: El Cerrito, California.

[15] Carr A. *Inelastic response spectra for the Christchurch earthquake records*: Christchurch, New Zealand, 2011. 120pp.

[16] Stirling MW, Gerstenberger M, Litchfield N, McVerry GH, Smith WD, Pettinga JR and Barnes P. *Updated probabilistic seismic hazard assessment for the Canterbury region*, 2007. 58pp.

[17] Beavan J, Fielding E, Motagh M, Samsonov S and Donnelly N. Fault Location and Slip Distribution of the 22 February 2011 Mw 6.2 Christchurch, New Zealand, Earthquake from Geodetic Data. *Seismological Research Letters* 2011; **82**(6): 789-799.

[18] Shahi SK and Baker JW. An Empirically Calibrated Framework for Including the Effects of Near-Fault Directivity in Probabilistic Seismic Hazard Analysis. *Bulletin of the Seismological Society of America* 2011; **101**(2): 742-755.

[19] Chiou B, Youngs R, Abrahamson N and Addo K. Ground-Motion Attenuation Model for Small-To-Moderate Shallow Crustal Earthquakes in California and Its Implications on Regionalization of Ground-Motion Prediction Models. *Earthquake Spectra* 2010; **26**(4): 907-926.

[20] Boore DM, Watson-Lamprey J and Abrahamson NA. Orientation-independent measures of ground motion. *Bulletin of the Seismological Society of America* 2006; **96**(4A): 1502-1511.

[21] Beyer K and Bommer JJ. Selection and scaling of real accelerograms for bi-directional loading: A review of current practice and code provisions. *Journal of Earthquake Engineering* 2007; **11**(1): 13-45.

[22] McVerry GH, Zhao JX, Abrahamson NA and Somerville PG. New Zealand acceleration response spectrum attenuation relations for crustal and subduction zone earthquakes. *Bulletin of the New Zealand Society for Earthquake Engineering* 2006; **39**(4): 1-58.

[23] Stewart JP, Abrahamson N, Atkinson GM, Baker JW, Boore DM, Bozorgnia Y, Campbell KW, Comartin CD, Idriss IM, Lew M, Mehrain M, Moehle JP, Naeim F and Sabol TA. Representation of bidirectional ground motion for design spectra in building codes. *Earthquake Spectra* 2011; **27**(3): 927-937.

[24] McVerry GH, Zhao JX, Abrahamson NA and Somerville PG. *Crustal and subduction zone attenuation relations for New Zealand earthquakes*, in *12th World Conference on Earthquake Engineering*: Auckland, New Zealand, 2000, 8pp.

[25] Abrahamson NA and Silva WJ. Empirical Response Spectral Attenuation Relations for Shallow Crustal Earthquakes. *Seismological Research Letters* 1997; **68**(1): 94-127.

[26] Youngs RR, Chiou S-J, Silva WJ and Humphrey JR. Strong Ground Motion Attenuation Relationships for Subduction Zone Earthquakes. *Seismological Research Letters* 1997; **68**(1): 58-73.

[27] Power M, Chiou B, Abrahamson NA, Bozorgnia Y, Shantz T and Roblee C. An overview of the NGA project. *Earthquake Spectra* 2008; **24**(1): 3-21.

[28] Pinheiro J, Bates DM, DebRoy S, Sarkar D and the R Core team. *nlme: linear and nonlinear mixed effects models*, 2008. pp.

[29] Abrahamson NA and Youngs RR. A stable algorithm for regression analyses using the random effects model. *Bulletin of the Seismological Society of America* 1992; **82**(1): 505-510.

[30] Webb T, Bannister S, Beavan J, Berryman K, Brackley H, Cousins J, Fry B, Gerstenberger M, Holden C, Kaiser A, McSaveney E, McVerry G, Pettinga J, Reyners M, Rhoades D, Somerville PG, Stirling MW, Van Dissen R, Villamor P, Wallace L and Zhao JX. *The Canterbury Earthquake sequence and implications for Seismic Design Levels*, 2011. 92pp.

[31] Abrahamson N. *Review of "The Canterbury Earthquake Sequence and Implications for Seismic Design Levels" dated July 2011.* , 2011. 19pp.

[32] Archuleta R. *Comments on "The Canterbury earthquake sequence and implications for seismic design levels"*, 2011. 12pp.

[33] Boatwright J. The Persistence of Directivity in Small Earthquakes. *Bulletin of the Seismological Society of America* 2007; **97**(6): 1850-1861.

[34] Somerville PG. Magnitude scaling of the near fault rupture directivity pulse. *Physics of The Earth and Planetary Interiors* 2003; **137**(1-4): 201-212.

[35] Bradley BA. A critical analysis of strong ground motions observed in the 4 September 2010 Darfield earthquake. *Soil Dynamics and Earthquake Engineering* 2012; (submitted).

[36] Bradley BA and Cubrinovski M. Near-source Strong Ground Motions Observed in the 22 February 2011 Christchurch Earthquake. *Seismological Research Letters* 2011; **82**(6): 853-865.

[37] Bradley BA and Cubrinovski M. Near-source strong ground motions observed in the 22 February 2011 Christchurch earthquake. *Bulletin of the New Zealand Society for Earthquake Engineering* 2011; (in press).

[38] Aagaard BT, Hall JF and Heaton TH. Effects of Fault Dip and Slip Rake Angles on Near-Source Ground Motions: Why Rupture Directivity Was Minimal in the 1999 Chi-Chi, Taiwan, Earthquake. *Bulletin of the Seismological Society of America* 2004; **94**(1): 155-170.

[39] Bradley BA and Cubrinovski M. Near-source strong ground motions observed in the 22 Febraury 2011 Christchurch earthquake. *Seismological Research Letters, Focused Issue on the 2011 Christchurch New Zealand Earthquake* 2011.

[40] Cubrinovski M, Bray JD, Taylor ML, Giorgini S, Bradley BA, Wotherspoon L and Zupan J. Soil liquefaction effects in the Central Business District during the February 2011 Christchurch earthquake. *Seismological Research Letters, Focused Issue on the 2011 Christchurch New Zealand Earthquake* 2011.

[41] Somerville PG, Smith NF, Graves RW and Abrahamson NA. Modification of empirical strong ground motion attenuation relations to include the amplitude and duration effects of rupture directivity. *Seismological Research Letters* 1997; **68**(1): 199-222.

[42] Hicks SR. *Structure of the Canterbury Plains, New Zealand from gravity modelling*, Geophysics Division, Department of Science and Industrial Research: Wellington, 1989. pp.

[43] Cubrinovski M and McCahon I. *Foundations on deep alluvial soils*, University of Canterbury, Christchurch, 2011. 40pp.

[44] Silva WJ. *Characteristics of vertical strong ground motions for applications to engineering design, FHWA/NCEER Workshop on the National Representation of*

Seismic Ground Motion for New and Existing Highway Facilities, Burlingame, CA, Proceedings, Earthquake Spectra, National Center for Earthquake Engineering Research: Buffalo, New York, 1997. pp.

[45] Bozorgnia Y and Campbell KW. The vertical-to-horizontal response spectral ratio and tentative procedures for developing simplified V/H and vertical design spectra. *Journal of Earthquake Engineering* 2004; **8**(2): 175-207.

[46] Kunnath SK, Erduran E, Chai YH and Yashinsky M. Effect of near-fault vertical ground motions on seismic response of highway overcrossings. *Journal of Bridge Engineering* 2008; **13**(3): 282-290.

[47] Choi Y, Stewart JP and Graves RW. Empirical Model for Basin Effects Accounts for Basin Depth and Source Location. *Bulletin of the Seismological Society of America* 2005; **95**(4): 1412-1427.

[48] Koketsu K, Hatayama K, Furumura T, Ikegami Y and Akiyama S. Damaging Long-period Ground Motions from the 2003 Mw 8.3 Tokachi-oki, Japan Earthquake. *Seismological Research Letters* 2005; **76**(1): 67-73.